AD-A053 431 COLD REGIONS RESEARCH AND ENGINEERING LAB HANOVER N H F/G 8/12
SOME ELEMENTS OF ICEBERG TECHNOLOGY,(U)
MAR 78 W F WEEKS, M MELLOR

UNCLASSIFIED CRREL-78-2 NL

1 OF 1
ADA
053431

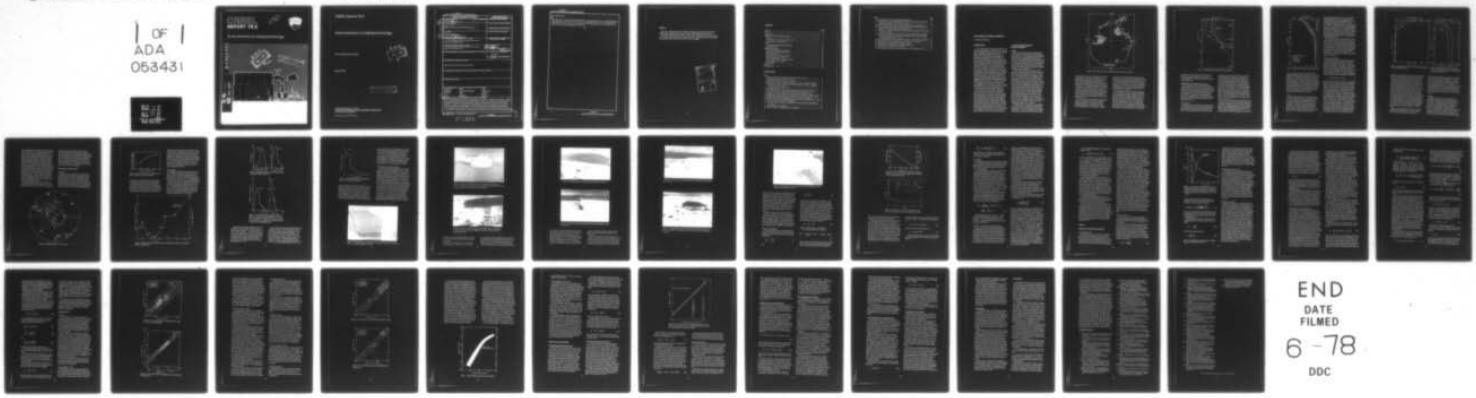

END
DATE FILMED
6-78
DDC

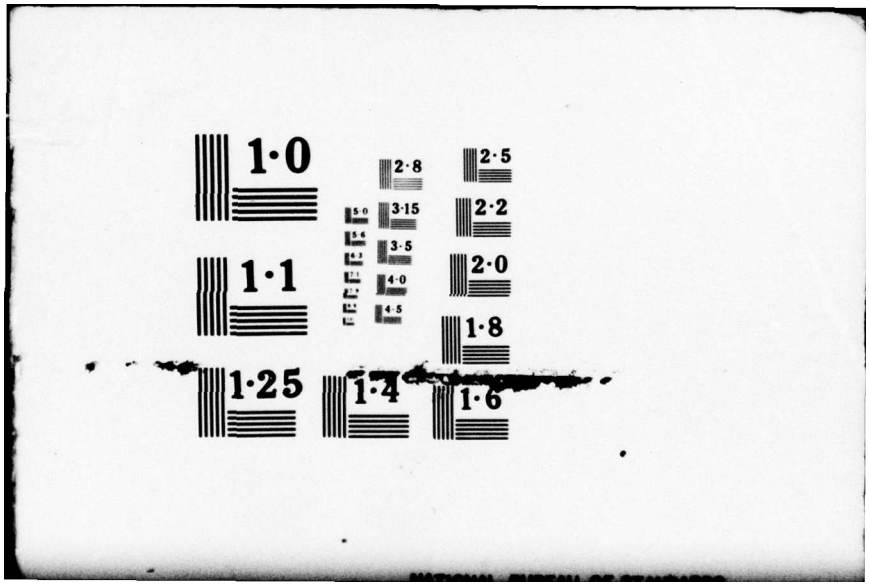
1·0
1·1
1·25
1·4
1·6
1·8
2·0
2·2
2·5
2·8
3·15
3·5
4·0
4·5

CRREL REPORT 78-2

12

Some elements of iceberg technology

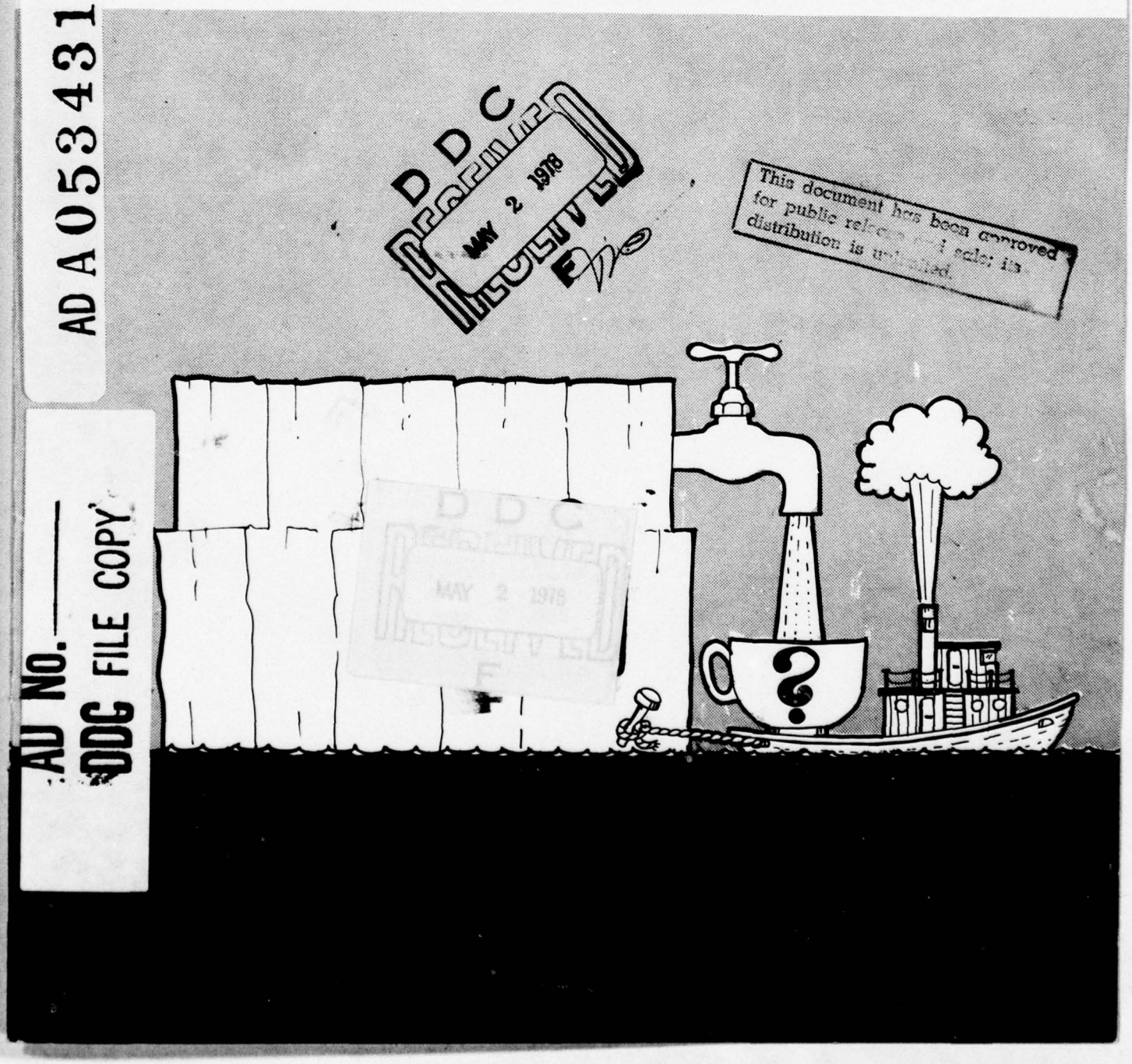

CRREL Report 78-2

Some elements of iceberg technology

W.F. Weeks and M. Mellor

March 1978

CORPS OF ENGINEERS, U.S. ARMY
COLD REGIONS RESEARCH AND ENGINEERING LABORATORY
HANOVER, NEW HAMPSHIRE

Unclassified

SECURITY CLASSIFICATION OF THIS PAGE *(When Data Entered)*

REPORT DOCUMENTATION PAGE

READ INSTRUCTIONS BEFORE COMPLETING FORM

1. REPORT NUMBER: CRREL [redacted]-78-2	2. GOVT ACCESSION NO.
3. RECIPIENT'S CATALOG NUMBER	
4. TITLE *(and Subtitle)*: SOME ELEMENTS OF ICEBERG TECHNOLOGY	5. TYPE OF REPORT & PERIOD COVERED
	6. PERFORMING ORG. REPORT NUMBER
7. AUTHOR(s): W.F. Weeks and M. Mellor Malcolm Mellor	8. CONTRACT OR GRANT NUMBER(s)
9. PERFORMING ORGANIZATION NAME AND ADDRESS U.S. Army Cold Regions Research and Engineering Laboratory Hanover, New Hampshire 03755	10. PROGRAM ELEMENT, PROJECT, TASK AREA & WORK UNIT NUMBERS
11. CONTROLLING OFFICE NAME AND ADDRESS U.S. Army Cold Regions Research and Engineering Laboratory Hanover, New Hampshire 03755	12. REPORT DATE: Mar[redacted]78 13. NUMBER OF PAGES: 37 (38 pp)
14. MONITORING AGENCY NAME & ADDRESS *(if different from Controlling Office)*	15. SECURITY CLASS. *(of this report)*: Unclassified 15a. DECLASSIFICATION/DOWNGRADING SCHEDULE

16. DISTRIBUTION STATEMENT *(of this Report)*

Approved for public release; distribution unlimited.

17. DISTRIBUTION STATEMENT *(of the abstract entered in Block 20, if different from Report)*

18. SUPPLEMENTARY NOTES

19. KEY WORDS *(Continue on reverse side if necessary and identify by block number)*

Cutting tools	Motion	Towing
Engineering	Performance (engineering)	Towing vehicles
Excavation	Ships	Tugboats
Ice	Stability	Underwater
Icebergs	Towed bodies	Velocity

20. ABSTRACT *(Continue on reverse side if necessary and identify by block number)*

Many of the technical questions relating to iceberg transport are given brief, but quantitative, consideration. These include iceberg genesis and properties, the mechanical stability of icebergs at sea, towing forces and tug characteristics, drag coefficients, ablation rates, and handling and processing the iceberg at both the pick-up site and at the final destination. In particular the paper attempts to make technical information on glaciological and ice engineering aspects of the problem more readily available to the interested planner or engineer. Specific conclusions include:
1) No unprotected iceberg, no matter how long or wide, would be likely to survive the ablation caused by a long trip to low latitudes. 2) Icebergs that have a horizontal dimension exceeding 2 km may well be prone to breakup by long

DD FORM 1 JAN 73 1473 EDITION OF 1 NOV 65 IS OBSOLETE

Unclassified

SECURITY CLASSIFICATION OF THIS PAGE *(When Data Entered)*

ϕ37100.

20. Abstract (cont'd)

wavelength swells. 3) To avoid the dangers associated with an iceberg capsizing, the width of a 200-m-thick iceberg should always be more than 300 m. 4) For towing efficiency the length/width ratio of a towed iceberg should be appreciably greater than unity. 5) For a pilot project, the selected iceberg would have to be quite small, if for no other reason than the practical availability of tug power.

PREFACE

This report was prepared by Dr. W.F. Weeks, Glaciologist, Snow and Ice Branch, Research Division, and Dr. Malcolm Mellor, Physical Scientist, Experimental Engineering Division.

The authors thank Stephen Ackley, Dr. Ian Allison, Dr. George Ashton and Dr. Andrew Assur for their advice, their data, and their general encouragement. Technical review of the manuscript was performed by Mr. Ackley and Dr. Anthony J. Gow of CRREL.

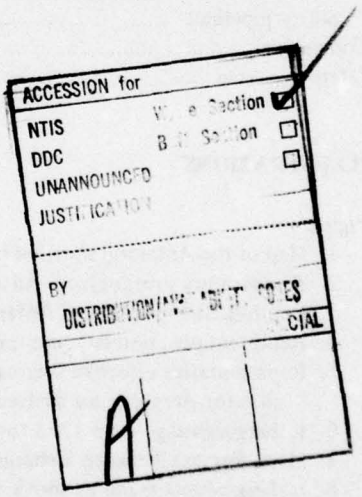

CONTENTS

ILLUSTRATIONS

SOME ELEMENTS OF ICEBERG TECHNOLOGY

W.F. Weeks and M. Mellor

INTRODUCTION

Around 1960, when we were first introduced to the idea of towing icebergs as a fresh water source, the idea seemed something of a joke. Since that time, technical papers by Weeks and Campbell[1] and Hult and Ostrander[2] have made preliminary appraisals of the problems and economics of tows to Australia and western South America and to California, respectively. Both studies concluded that the idea appeared to have merit and might be possible, and recommended further exploratory studies. In the intervening period, this idea has come to be taken very seriously inasmuch as pure ice is potentially a very valuable natural resource and problems caused by a shortage of water are being encountered at a rapidly increasing number of locations throughout the world. Tows have even been contemplated to such difficult locations as the Red Sea.[3] The interest in iceberg towing has reached the point where a suggestion has been made that a pilot program should be undertaken in the near future.[3 4] However, it should be remembered that most of the technical studies recommended by the 1973 papers[1 2] have not yet been undertaken, and some technical problems that may well be critical have been almost completely ignored.

Here we attempt to review some of the technical factors involved in iceberg towing in a simple but quantitative manner. The aim is to provide pertinent technical data that can be used in a balanced appraisal of the overall problem. This effort was prompted by what appeared to be misconceptions concerning the nature of tabular Antarctic icebergs and the engineering problems involved in transporting them. Although the literature on glaciology tends to be hidden in somewhat obscure nooks and crannies, it does exist, and there is considerable information that has direct bearing on the problem of iceberg towing. We hope that this paper will provide a key to some of this information.

SOURCES AND PROPERTIES OF TABULAR ICEBERGS

Sources

When "towing" a large iceberg a long distance is being considered, the initial shape of the iceberg seems quite important. If the iceberg is tabular the problems associated with rolling and tipping during the tow should not become significant until the iceberg has been extensively modified by melting. The prime sources of such icebergs are the great ice shelves of the Antarctic. There are also tabular icebergs in the North Atlantic, but they are neither common nor large when compared with their Antarctic equivalents.

The Antarctic ice shelves are floating ice sheets generally occupying large embayments that form more than one-third of the Antarctic coastline.[5] They are fed at their landward edges by ice discharged by land glaciers, and nourished at their upper surfaces by the accumulation of snow. At most locations near the seaward edges of the shelves the accumulation of snow appears to be the predominant factor. Many ice shelves are confined within flanking arms of either land or inland ice, with the shelf ice gradually flowing from the thicker landward portions of the shelves outward toward the thinner seaward edges. The seaward edges of the ice shelves are commonly marked by vertical cliffs ranging in height from a few meters to 50 m. Representative values appear to lie between 30 and 40 m. A total ice thickness of 200 m is commonly assumed to be the equilibrium value at sites near the ice edge. Estimates of ice shelf velocities vary widely, ranging from roughly 0.3 to 2.6 km/yr.[5]

Crevasses appear to be relatively rare in ice shelves except where major ice streams enter, where shelves are grounded, or where the floating ice shears against land-based ice. However, crevasses do occur near the seaward edges of the shelves and radioecho sounding

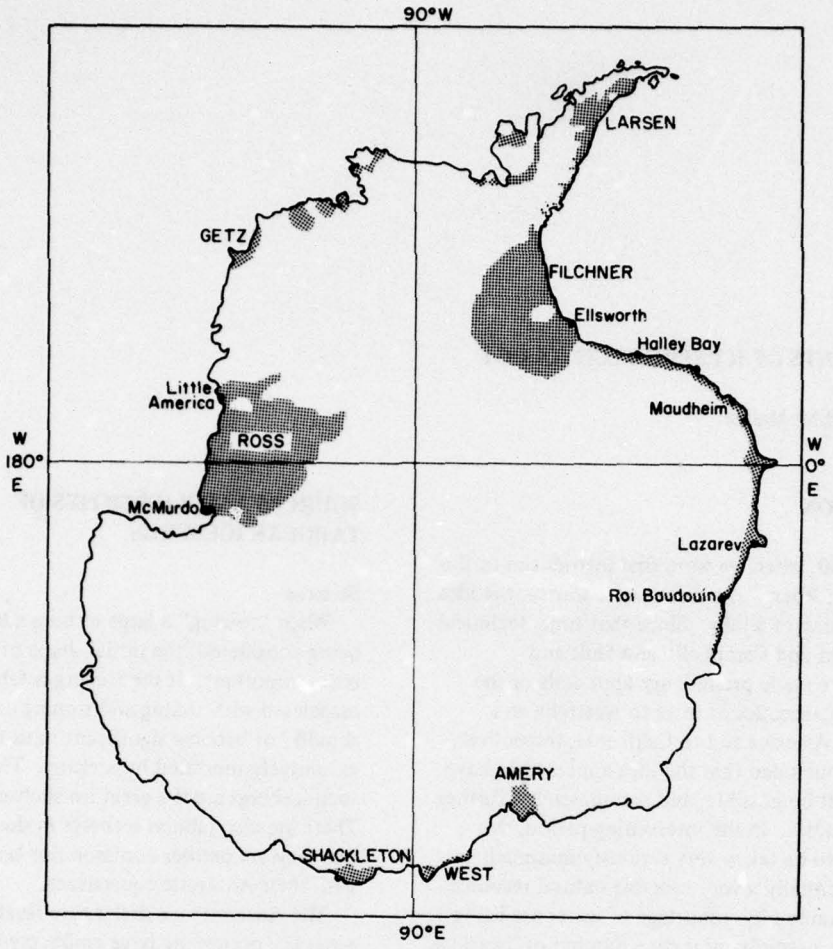

Figure 1. Map of the Antarctic showing the location of the major ice shelves.

has revealed some "bottom" crevasses that open downward without an obvious surface expression. Very little is known about either the calving process or its timing. The few glaciologists who have become involved in the calving process do not recommend close participation.[6] Although iceberg generation is usually considered to be a reasonably continuous process when viewed on a time scale of a year or more, there are documented cases when large areas of a given ice shelf calved within a short period of time. For instance in 1963 one fifth of the Amery Ice Shelf (9600 km^2 or approximately 40 years growth) broke off and drifted away to the west.[7]

Figure 1 is a map of the Antarctic showing the locations of the major ice shelves. Their total area is roughly 1,400,000 km^2. The largest is the Ross (530,000 km^2), which is followed in size by the Filchner (400,000 km^2). Of the smaller ice shelves (in area) the Amery is probably the most important inasmuch as it is fed by the Lambert Glacier, an immense ice stream whose drainage basin comprises about 1/8 of the total area of Antarctica. Estimates of the annual output of ice from this one ice shelf[7] are approximately 31,000 million m^3. An estimate of the overall annual shelf iceberg "export" from the Antarctic[8] is of the order of 10^{12} m^3, or 10^3 km^3.

At the present time there is no basis for suggesting that the properties of tabular icebergs from one shelf are more desirable than those of icebergs from another. But the locations of the different shelves, when considered in conjunction with the patterns of the most favorable ocean currents, do tend to couple specific shelves with specific delivery sites. For instance ice from the Amery, West, and Shackleton Shelves would presumably favor towing to Australia; ice from the Ross Shelf towing to the Atacama Desert and to California;

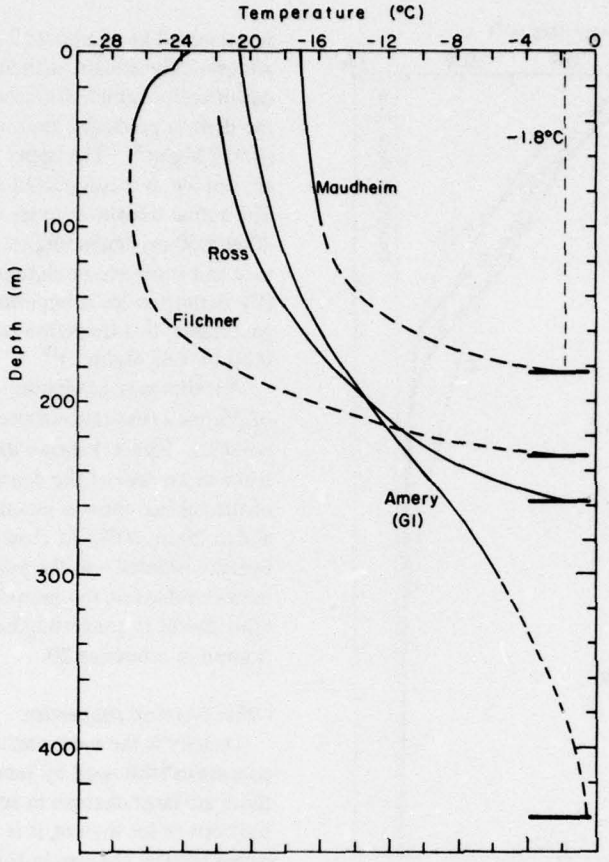

Figure 2. Temperature profiles from Antarctic ice shelves.

and ice from the Larsen and Filchner Shelves and the Queen Maud Land Coast (the stretch of shelf from roughly Halley Bay to Roi Baudouin) to Western Africa and the Middle East.

Characteristics of ice shelves near the ice front

We are not aware of any studies of the physical or chemical properties of the ice in actual tabular Antarctic icebergs. There are, however, a few studies of the nature of the ice in Antarctic ice shelves at locations near their seaward edges. The ice properties observed at these sites would not be expected to change significantly when the ice studied becomes part of a tabular iceberg, although there will obviously be changes when the iceberg moves out to sea.

Ice temperatures

At the snow-covered surfaces of the ice shelves there are fluctuations in the snow temperatures that generally follow the seasonal variations in the ambient air temperature. With increasing depth in the ice sheets these temperature fluctuations rapidly damp out, and the snow temperature at a depth of 10 m gives a good measure of the mean annual surface temperature. A map of estimated mean annual surface temperatures for Antarctica based mainly on 10-m snow temperatures can be found in reference 9. Temperatures near the edges of the ice shelves lie in the following ranges: Ross, −24 to −27°C; Filchner, −23 to −25°C; and the Queen Maud Land Coast, −10 to −18°C. There have been no 10-m temperatures published for sites near the edge of the Amery Ice Shelf, but existing temperature patterns[9] and unpublished data[10] for site G1, located 60 km from the coast, suggest that the values are in the range of −15 to −17°C.

Below 10 m there is, in general, a gradual increase in ice temperature, with the observed values slowly approaching the freezing temperature of sea water (−1.8°C for normal salinities at 1 atmosphere pressure) at the base of the shelf. Figure 2 shows the available profile data for the Amery, Filchner, Ross, and Maudheim ice shelves.[10 11 12 13] The striking nonlinearity of the temperature profiles between

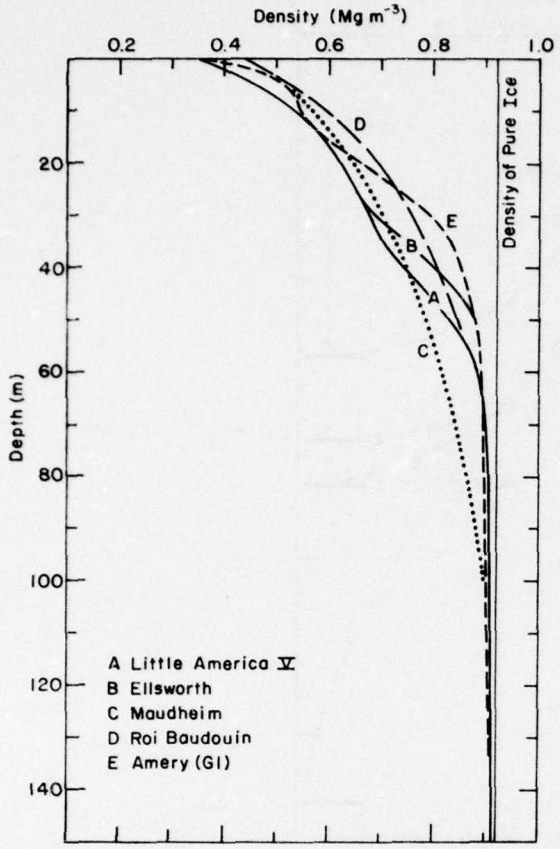

Figure 3. Depth-density profiles of Antarctic ice shelves.

10 m and the shelf base on the Filchner, Ross and Maudheim Shelves is believed to be the result of bottom melting.[14 15] The Amery temperature profile, which is quite different from the others in shape, is from much thicker ice (440 m) at a location approximately 60 km from the shelf edge where bottom ice growth is believed to have been significant.[10] The negative "bulge" in the Filchner profile is presumed to be caused by the rapid advection of cold ice. These profiles show that at the time of calving a tabular Antarctic iceberg can be expected to have a significant "cold reserve."

Density

A map showing the density of the uppermost 2 m of snow at a wide variety of sites in the Antarctic can be found in reference 9. Representative values for near-coastal ice shelf sites lie in the range of 0.35 to 0.42 Mg/m^3. The same reference summarizes snow densities at 10-m depth which range between 0.53 and 0.59 Mg/m^3. Figure 3 shows the five depth-density profiles that have been determined at ice shelf sites.[10 11 13 16 17] Much of these data are also summarized in references 9 and 18. All the profiles are generally similar, with an initially high rate of densification which decreases at depths below 60 m as the density gradually approaches that of pure ice (0.917 Mg/m^3). The upper portions of tabular icebergs are not ice, but compacted snow, which is permeable. The actual transition to ice occurs at depths of between 40 and 60 m, depending on the mean annual temperature and snow accumulation rate at the site in question. (By definition ice is impermeable to air while snow is permeable; this transition occurs in the density range 0.80 to 0.83 Mg/m^3.)[19]

Another way of viewing density profiles is in terms of porosity (the ratio of the void volume to the total volume). Figure 4 shows the porosity profile derived from an average of the density profiles. The porosity of the surface snow is just under 60%, at 10 m it is 39%, and at 20 m, 30%. At close-off, when the air bubbles become isolated and the permeable snow changes to impermeable ice, the porosity is roughly 10%.[19] A table useful in converting between density and porosity is given in reference 20.

Other physical properties

Density is the most useful single indicator of snow properties (followed by temperature). Inasmuch as there are large changes in snow density in the upper portions of ice shelves, it is reasonable to expect appreciable vertical changes in the physical properties of tabular icebergs. To illustrate this, Figure 4 gives a plot of the specific permeability of a tabular iceberg as a function of depth. The values of specific permeability (k) were obtained from the relation given by Shimizu:[21]

$$k = 0.077\, d^2 \exp(-7.8\, \rho_s/\rho_w) \qquad (1)$$

where d is the mean grain size and ρ_s/ρ_w is the specific gravity of the snow. [The units of k are controlled by the units used for d (if d is specified in mm, k will be in mm^2).] In estimating k it was assumed that d has a constant value of 1 mm. In fact, grain sizes at depth may be appreciably larger than this value.[9 22] However, large crystals usually occur at depths where the ice is impermeable. It might be noted that the specific permeability parameter applies to the movement of any fluid through the snow; the permeability of a specific fluid can be obtained by dividing k by the dynamic viscosity of the fluid in question. The upper portion of the iceberg is highly permeable. This should be taken into account if one proposes to store water in a lake formed on the upper surface of an iceberg. The fact that the upper 50 m of a tabular iceberg is permeable is also important in that once an iceberg has drifted far enough to the north so that melting occurs at its

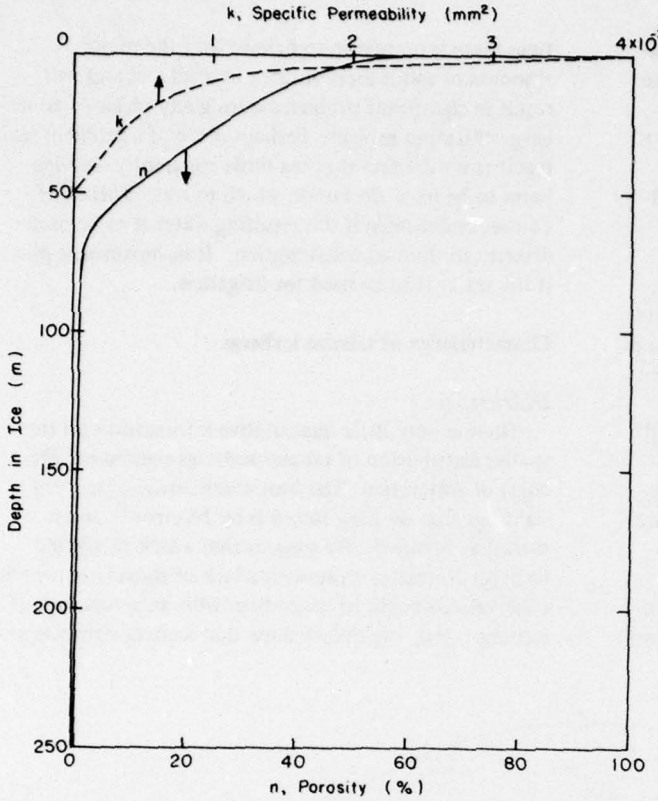

Figure 4. Representative porosity and specific permeability profiles for Antarctic ice shelves.

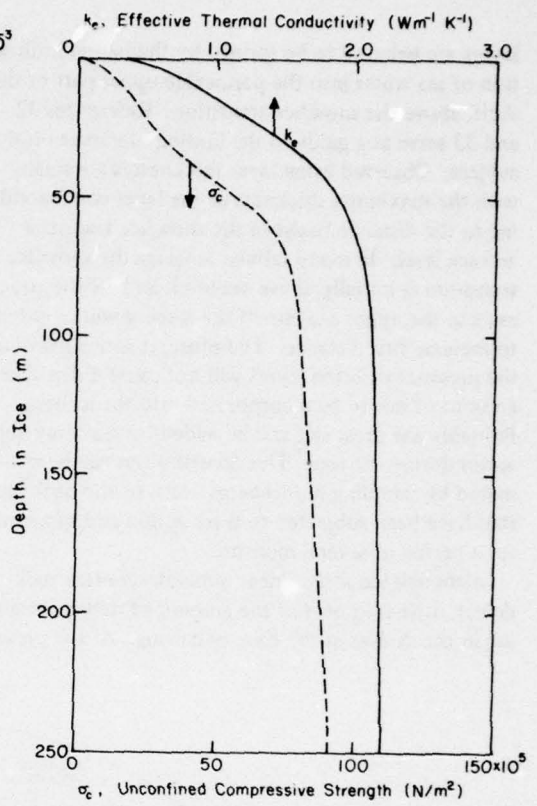

Figure 5. Representative effective thermal conductivity and uniaxial compressive strength profiles for Antarctic ice shelves.

upper surface the meltwater will percolate down through the snow. Upon refreezing the melt water will release its latent heat, producing an increase in snow temperature until the iceberg at depths above the snow/ice transition becomes isothermal at 0°C. This process has been well documented on glaciers and ice sheets[23] and is very efficient compared to conductive processes which would predominate below the snow/ice transition. Therefore, during a considerable portion of a tow to lower latitudes, the upper part of the iceberg would probably consist of water-saturated snow, a material whose properties are not well understood. It also should be remembered that when water flows through an isothermal snowpack at 0°C, any excess heat will result in ice melting, which will in turn increase the permeability, resulting in more rapid movement of water, more melting of ice, and so on. This translates into "small leaks in water-saturated snowpacks rapidly become large leaks."

Figure 5 shows representative profiles of two other parameters of potential interest, the thermal conductivity and the uniaxial compressive strength.[24,25] Again, large variations can be expected in the upper 50 m of the ice shelf. Similar plots might have to be prepared for other parameters. References 24, 26 and 27 and 28-30 are useful guides to published work on the physical properties of snow and ice, respectively. In applying published values to Antarctic shelf ice problems, care should be taken to ascertain that the values used were determined on ice that was similar in structure as well as in temperature and density to the ice at the site of interest.

Impurities

In general, snow and ice from the Antarctic are chemically extremely pure, with conductivities of 1 to 2 μmhos/cm, corresponding to good quality distilled water. Even at coastal sites such as Little America V the maximum conductivity observed was only 49 μmhos/cm, corresponding to excellent quality raw water.[31] There are, however, brine layers that are known to occur in ice shelves near McMurdo, Brunt, Lazarev and Wilkes and, based on radio echo sounding, are presumed to occur in the Wordie and Larsen shelves. These

layers are believed to be formed by the lateral infiltration of sea water into the permeable upper part of the shelf, above the snow/ice transition. References 32 and 33 serve as a guide to the limited literature on this subject. Observed brine layer thicknesses are small, with the maximum thickness of the layer corresponding to the distance between the snow/ice transition and sea level. In many tabular icebergs the snow/ice transition is initially above sea level, and erosive processes in the upper portion of the iceberg will only tend to increase this distance. Therefore, it seems likely that the presence of brine layers will not cause a significant amount of salt to be incorporated into the iceberg. Probably the most salt will be added by sea spray and waves during the tow. This contribution can be estimated by sampling old icebergs north of the pack ice that have been subjected to wave action and salt spray for a period of several months.

Although ice shelves near nunataks contain rock debris, little is known of the amount of debris remaining in the shelves at the time of calving. At the present time there is no reason to believe that the minor amounts of solids incorporated in shelf icebergs will result in significant problems during any phase of an iceberg utilization project. Perhaps more of a problem will result from the fact that sea birds apparently find icebergs to be ideal sites upon which to rest. This is, of course, undesirable if the resulting water is to be used directly for human consumption. It is, however, a plus if the water is to be used for irrigation.

Characteristics of tabular icebergs

Distribution

There is very little quantitative information on the spatial distribution of tabular icebergs sighted off the coast of Antarctica. The best compilation of iceberg sightings that we have found is by Nazarov[34] and is shown as Figure 6. We suspect that a lack of sighted icebergs correlates more with a lack of ships from which observations could be made than with an actual lack of icebergs. Nazarov's plots show that iceberg sightings are

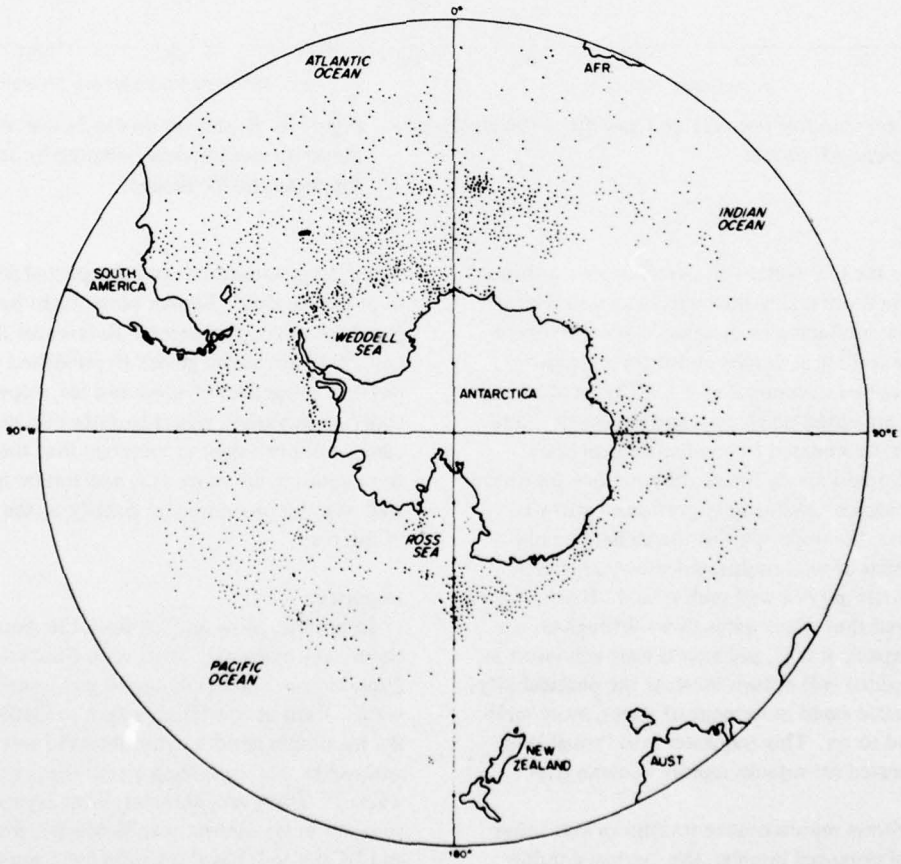

Figure 6. Iceberg sightings from 1773 to 1960.[34]

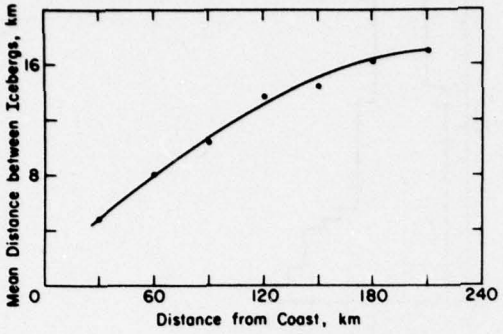

Figure 7. Mean distance between icebergs versus distance from the coast of East Antarctica.[35]

common as far north as 40°S in the South Atlantic and Indian Oceans and to 50°S in the South Pacific.

In general, there are large numbers of icebergs located near the Antarctic continent and a gradual decrease further north. This trend is shown in Figures 7 and 8. Figure 7, which is a replot of data presented by Gordienko,[35] shows a gradual increase in the mean distance between icebergs as one moves off the coast of East Antarctica. Figure 8, which is based on results provided by S. Ackley of CRREL, shows a similar decrease in iceberg frequency as one moves north in the Weddell Sea. If the iceberg frequencies for the Weddell Sea are converted into mean spacings between icebergs, the values obtained vary from 5.5 to 18.5 km, in the same range as the results of Gordienko.[35] (Here we exclude the one reading at 67°S where almost no icebergs were sighted by Ackley.)

Size and shape

Surprisingly little quantitative information is available on the sizes and shapes of tabular Antarctic icebergs. Some are very large, the largest reported one being 185 km on one side.[5] Other large icebergs have had dimensions of 140×60 km,[36] 100×70 km and 100 ×45 km.[37] The latter two icebergs, although sighted in the Weddell Sea, apparently originated from the Amery Ice Shelf, and they are believed to have drifted a distance of roughly 4000 km along the Antarctic coast over a period of 6 years. Although such immense icebergs are of considerable interest and can readily be tracked by meteorological satellites (cloud cover permitting), towing them is out of the question.

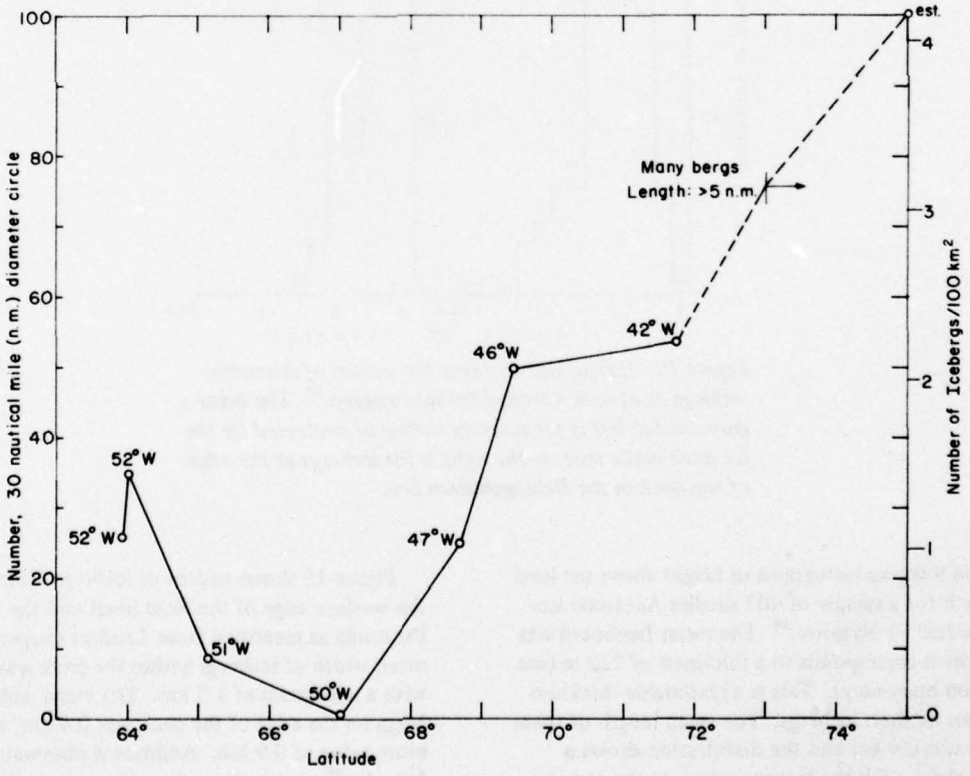

Figure 8. Iceberg counts made by ship's radar in the Weddell Sea in February 1977 (Ackley, personal communication).

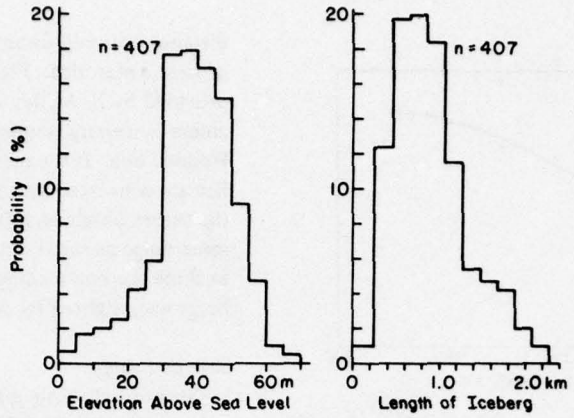

Figure 9. Histograms showing the freeboard and lengths of icebergs studied by Nazarov.[34]

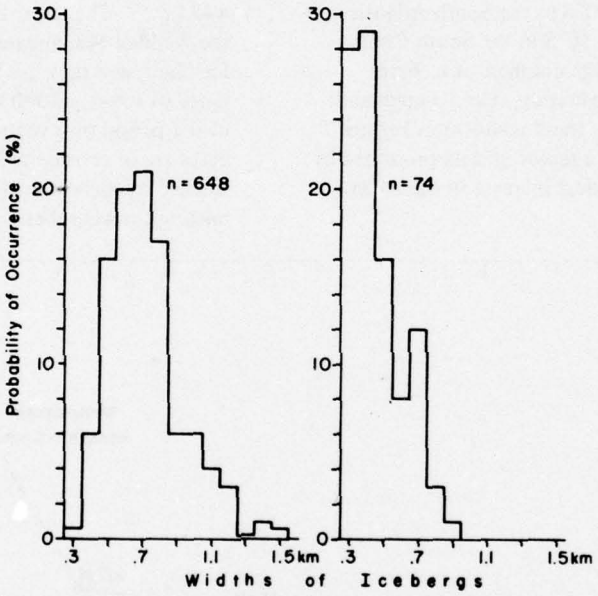

Figure 10. Histograms showing the widths of Antarctic icebergs as observed from Landsat imagery.[38] *The histogram on the left is for icebergs within or protected by the ice pack while that on the right is for icebergs at the edge of the pack in the Bellingshausen Sea.*

Figure 9 shows histograms of height above sea level and length for a sample of 407 smaller Antarctic icebergs studied by Nazarov.[34] The mean freeboard was 40 m, which corresponds to a thickness of 222 m (see section on buoyancy). This is a reasonable thickness for Antarctic shelf icebergs. The mean length of these icebergs was 0.9 km and the distribution shows a positive skew, with the largest iceberg in the sample having a length of 2.3 km.

Figure 10 shows widths of icebergs observed between the western edge of the Ross Shelf and the Antarctic Peninsula as measured from Landsat imagery.[38] The mean width of icebergs within the pack was 0.7 km with a maximum of 1.5 km. The mean width of icebergs on the edge of the pack was 0.4 km, with a maximum value of 0.9 km. Additional observations by Lebedev[39] on tabular iceberg dimensions found at or north of the pack ice edge give lengths between 0.1 and

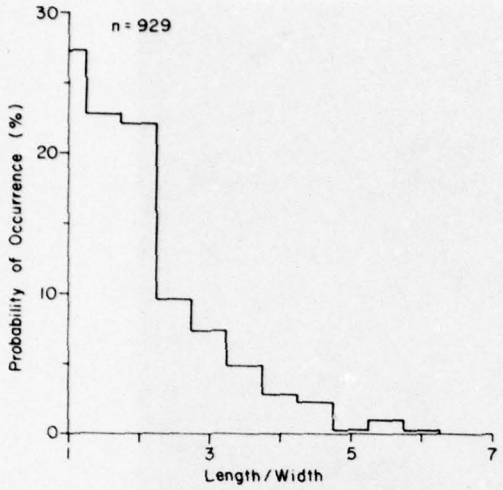

Figure 11. Histogram showing observed length to width ratios for Antarctic icebergs.[34]

0.4 km and freeboards between 12 and 40 m. It is at present not possible to rule out the chance that these differences in iceberg characteristics are the result of different source areas for the icebergs. However, this seems unlikely. We agree with Kovacs'[40] suggestion that these differences are telling something that must be heeded in any successful iceberg towing scheme: that once tabular icebergs are subjected to high waves, they tend to break up to a stable size which is largely determined by their thickness and the nature of their defects, and they are also subject to rapid erosion.

The only set of systematic data on the length to width ratios of Antarctic icebergs is also found in Nazarov (his Fig. 13). Figure 11 is based on these data and it shows that most icebergs have length to width ratios between 1 to 1 and 2 to 1, and that length to width ratios of 5 to 1 or greater are not common.

Iceberg surfaces and erosive processes

At the time of calving the upper surfaces of tabular icebergs are flat, featureless expanses of snow. This is illustrated in Figure 12, which shows an iceberg that might be considered ideal for towing, and in Figure 13, which shows a helicopter sitting on a tabular iceberg in the Weddell Sea. Other views of the upper surfaces of such icebergs can be seen in Figures 14-17. Because of the snow cover, flaws such as cracks or crevasses may not be readily identifiable by simple visual examinations of the upper surface (see Fig. 13). Thus remote sensing techniques may be useful in selecting icebergs suitable for towing. As the iceberg encounters above-freezing air temperatures, its upper surface would gradually become wet snow. At some locations snow swamps might develop. Once water starts to drain from the iceberg surface, a drainage pattern should develop quite rapidly. The lower surfaces of shelf icebergs are in general believed to be quite flat, based on radioecho

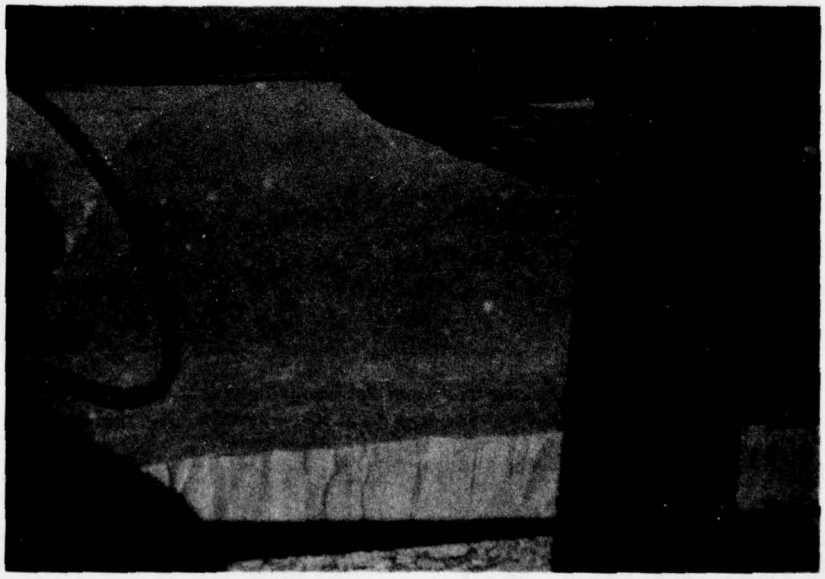

Figure 12. Tabular iceberg in the Weddell Sea with horizontal dimensions of approximately 1×6 km (photograph by S. Ackley).

Figure 13. The top of a tabular iceberg in the Weddell Sea (photograph by S. Ackley). Although it is not apparent in this photograph, a small crevasse runs across the surface between the helicopter and the photographer.

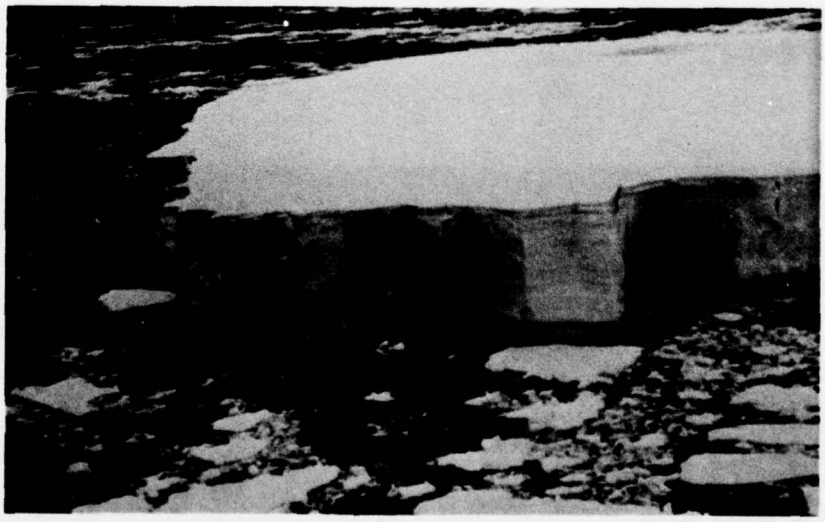

Figure 14. Crevasses in a tabular iceberg in the Weddell Sea that have apparently been widened by wave action (photograph by S. Ackley). Note also the wave-induced undercutting.

sounding. However, detailed examinations of the bottom surfaces of actual icebergs are only now starting to be made.[40]

Figures 12 and 15-18 show views of the sides of tabular icebergs. Although these sides are initially vertical walls at the time of calving (see Fig. 12 and 15), they rapidly become modified by a process in which the higher local water velocities produced by wave action cause higher effective heat transfer rates between the ice and the near-surface water, resulting in rapid melting.

Figure 15. Tabular iceberg in the Weddell Sea (photograph by S. Ackley).

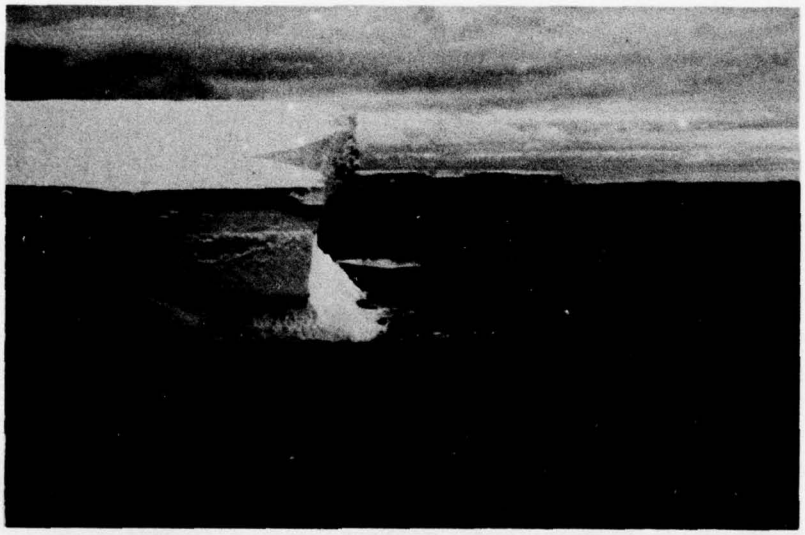

Figure 16. View of the sides of a tabular iceberg in the Weddell Sea (photograph by S. Ackley).

This results in localized undercutting of the vertical walls of the above-water portions of the icebergs, with their subsequent failure and collapse into the sea. Evidence of undercutting and overhanging ice cliffs is displayed in Figures 14, 16, 17 and 18. The stratified nature of the upper portions of shelf icebergs can clearly be seen in Figures 16 and 17. The instability of these ice cliffs should be considered in any scheme to protect an iceberg from thermal erosion, and the hazard to people and equipment should be fully appreciated.

Little is known about the underwater portions of the sides of tabular icebergs. There is usually a "terrace" projecting out just below the waterline. This results from cliff erosion produced by undercutting caused by wave-enhanced melting. Figure 19 is a close-up of the

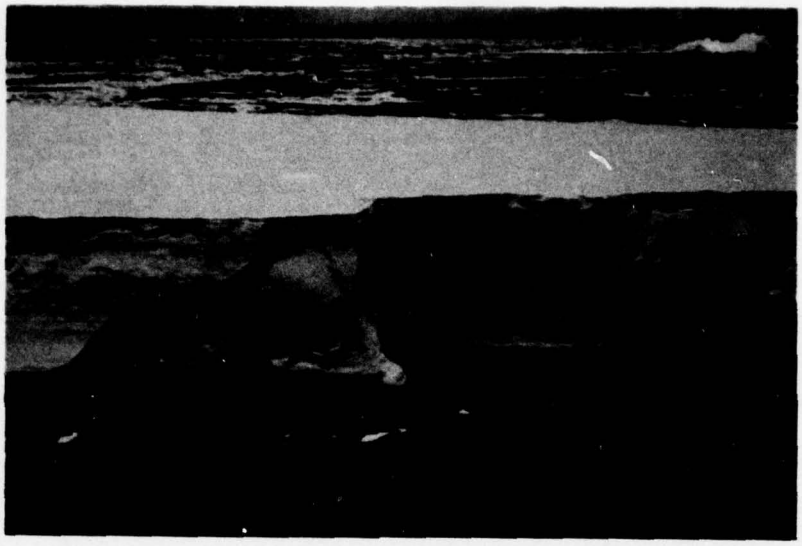

Figure 17. View of the side of a tabular iceberg in the Weddell Sea (photograph by S. Ackley).

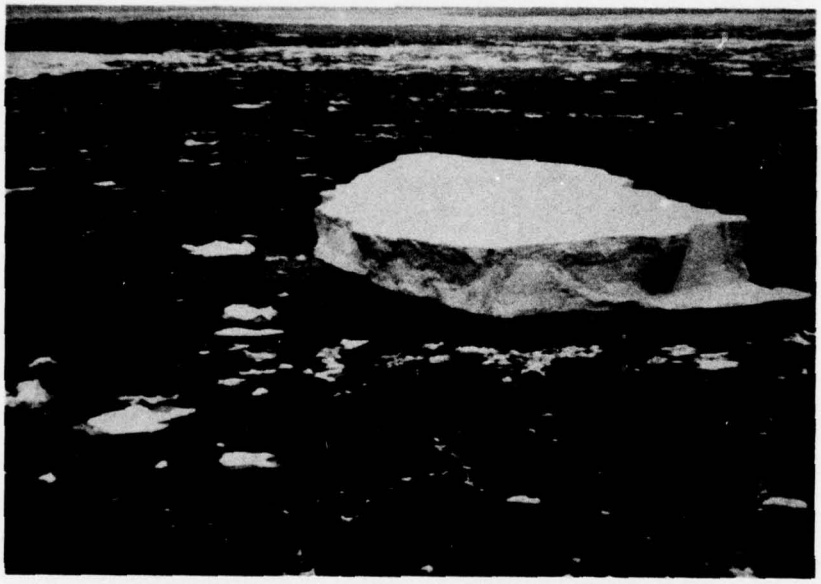

Figure 18. A small tabular iceberg in the Weddell Sea showing a raised wave-cut terrace on the right and a submerged wave-cut terrace on the left (photograph by S. Ackley).

Figure 19. Close-up of the wave-cut terrace shown in the right-hand portion of Figure 18 (photograph by S. Ackley).

wave-cut terrace that appears in the right-hand portion of Figure 18. The terrace here is exposed because of tilting caused by uneven erosion of the iceberg. Note that the terrace on the left-hand portion of the iceberg shown in Figure 18 is under water. Such tilting, which presumably occurs quite rapidly, would have striking effects on any shallow lake that might have been formed on the upper surface of a tabular iceberg. We are not aware of any detailed observations on the nature of the iceberg surfaces below the wave-cut terrace.

It might be noted that wave-induced thermal erosion has probably had a major role in enlarging the crevasses shown in Figure 14. In fact, if there is any flaw in an iceberg, wave-induced erosion is likely to find it and rapidly enlarge it. An impression of how efficient this process is can be gained from reference 41, which describes the break-up of a large tabular iceberg northeast of the Grand Banks of Newfoundland.

Buoyancy considerations

The draft and freeboard of a wide berg depend on the densities of the ice and the water. If the total ice thickness is T and the freeboard and draft are h_1 and h_2 respectively

$$\frac{h_1}{T} = 1 - \frac{\bar{\rho}_i}{\rho_w} \tag{2}$$

and

$$\frac{h_1}{h_2} = \frac{\rho_w}{\bar{\rho}_i} - 1 \tag{3}$$

where $\bar{\rho}_i$ is the mean density of the ice and ρ_w is the mean density of seawater down to depth h_2. The density of cold seawater can be taken as 1.03 Mg/m^3. However, the mean density of the ice depends on the depth-density profile. As was shown earlier, the upper part of the depth-density curve is more or less the same, irrespective of total depth, so that the effect of low densities in the uppermost layers becomes progressively less significant as T increases. For present purposes, it can be assumed that the density defect of the upper layers in a "dry" ice shelf is equivalent to a layer of solid ice about 16 m thick. Thus

$$\bar{\rho}_i = \rho_i (1 - 16/T) \tag{4}$$

where T is in meters and $\rho_i \approx 0.91$ Mg/m^3.

For a wide tabular berg with vertical sides

$$\frac{h_1}{T} = 1 - \left(\frac{\rho_i}{\rho_w}\right)(1 - 16/T) = 1 - 0.883\,(1 - 16/T). \tag{5}$$

Figure 20 shows how the freeboard and draft of a wide, uniform berg vary with total thickness. In this paper, most of the calculations assume a total thickness of

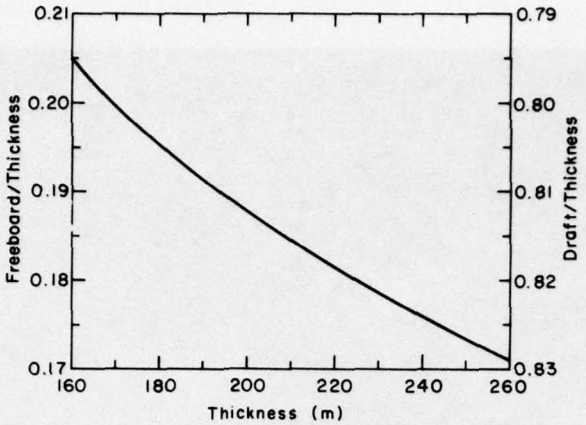

Figure 20. Plot of the change in the freeboard to thickness and draft to thickness ratios with a change in the total thickness of Antarctic shelf icebergs.

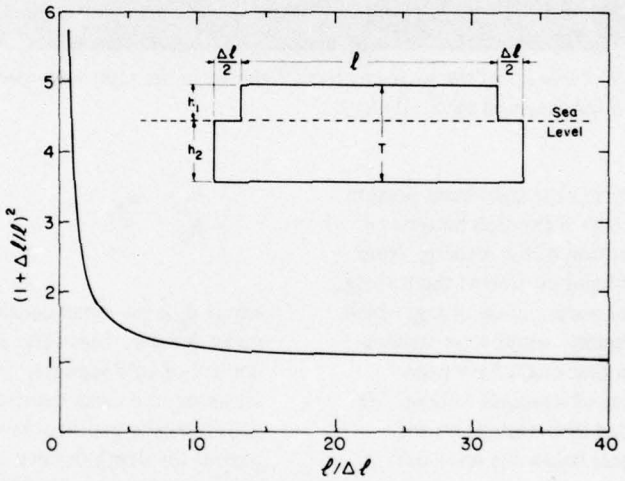

Figure 21. The factor $[1 + (\Delta\ell/\ell)]^2$ which gives the adjustment for the presence of wave terraces as a function of $\ell/\Delta\ell$.

200 m, for which the freeboard is 18.8% of the thickness and the draft is 81.2% of the thickness.

Small tabular icebergs sometimes ride higher in the water than wide bergs because of the wave terrace formed by cliff erosion (this is quite important for very small "ice islands" in the Arctic). The effect of this buoyancy change can be assessed by assuming that the wave terrace is a uniform rectangular notch in the edge of a uniformly thick berg, as shown in Figure 21. The linear dimension ℓ characterizes the size of the iceberg, such that the area of its top is $k\ell^2$, where k is a shape factor (e.g. $k = \pi/4$ for a circular berg or k is the length/breadth ratio for a rectangular berg). The horizontal dimension below the waterline exceeds ℓ by an amount $\Delta\ell$, giving a terrace width of $\Delta\ell/2$ at the waterline. If $\kappa \approx 1$ or $\ell >> \Delta\ell$, the volume of the berg V_i is

$$V_i = k h_1 \ell^2 + k h_2 (\ell + \Delta\ell)^2 \qquad (6)$$

and the volume of water displaced, V_w, is

$$V_w = k h_2 (\ell + \Delta\ell)^2. \qquad (7)$$

Taking a single approximate value of mean ice density $\bar{\rho}_i$ in accordance with eq 4, the freeboard to draft ratio becomes

$$\frac{h_1}{h_2} = \left(1 + \frac{\Delta\ell}{\ell}\right)^2 \left(\frac{\rho_w}{\rho_i} - 1\right) \qquad (8)$$

where the factor $[1 + (\Delta\ell/\ell)]^2$ is the adjustment for the effect of wave terraces. Numerical values of the factor are given in Figure 20.

Roll stability

If the berg is too narrow it will be in danger of rolling over. The minimum requirement is that the metacentric height should be positive, but it would be more reasonable to require a metacentric height at least equal to 10% of the berg width.

If the total thickness of the berg is T, the draft can be taken approximately as $0.81T$ (see *Buoyancy considerations*), and the depth to the center of buoyancy (from the waterline) as $0.405T$. Because density increases with depth in the berg, the center of gravity is not exactly at mid-depth, but rather at a depth $(T/2) + \Delta$. The increment Δ is actually a weak function of T, but for present purposes a constant value of $\Delta = 6$ m can be taken (this is actually for $T = 200$ m, but it does not vary by more than ± 10% for $130 < T < 260$). Thus the depth of the center of gravity from the berg surface is $(T/2) + 6$ m, where T is in meters.

The vertical distance between the center of buoyancy and the center of gravity is $0.095T + 6$ m. The volume of water displaced per unit length is $0.81BT$, where B is the berg width (assumed uniform). The moment of inertia of the section (per unit length) is $B^3/12$. Hence the metacentric height H_m is

$$H_m = \frac{B^3}{12 \times 0.81BT} - (0.095T + 6) \quad \text{m}$$

$$= \frac{B^2}{9.72T} - 0.095T - 6 \quad \text{m.} \qquad (9)$$

The minimum requirement is for $H_m > 0$, and a more conservative requirement is for $H_m \geq 0.1B$. Taking $T = 200$ m, the berg should be at the very least 220 m wide, and preferably 320 m wide, to avoid the danger of rolling over.

Wave flexure in ice shelves and tabular icebergs

Flexure caused by ocean waves may well influence, or perhaps even control, the calving of bergs from ice shelves and the mechanical breakup of large tabular bergs. When simple water waves travel beneath a floating elastic plate, the plate tends to flex in response to wave action. If the plate is very thin relative to the wavelength, and if wave amplitude is much smaller than the wavelength, then the plate will tend to bend without breaking. By contrast, if the plate is very thick relative to the wavelength it will not experience any significant flexure. Between these extremes there is a critical wavelength that maximizes the transient flexural stresses in the plate for any given wave amplitude.

The required analysis is one dealing with flexure of elastic beams on an elastic foundation. For the ice shelf calving problem, the free edge condition calls for treatment of a semi-infinite beam or plate. For the free-floating iceberg, the analysis ought to deal with a finite beam or slab. In preparing this paper we have not had time to trace or derive such analyses, but solutions for the infinitely extended plate were obtained by Assur,[42] who was concerned with wave cracks in sea ice (similar ideas are involved in the analysis of traveling loads on floating ice). For a preliminary analysis, the infinite plate treatment is probably sufficient to indicate general magnitudes for critical wavelengths and stresses, although it will probably underestimate stresses for the iceberg problem.

Assur's analysis deals with flexure of a wide elastic beam that floats on water and is displaced by non-attenuating sinusoidal waves of single frequency. Inertial effects are neglected, since the waves are "slow." The ice is assumed to have uniform properties from top to bottom. Wavelength and wave amplitude are treated as mutually independent variables.

For the infinite plate, the critical wavelength L_* that maximizes the "extreme fibre" stresses σ at constant wave amplitude A is

$$L_* = \pi \left[\frac{8Eh^3}{3k(1 - \mu^2)}\right]^{1/4} \qquad (10)$$

where E is Young's modulus, h is ice thickness, k is the foundation modulus (unit weight of water), and μ is Poisson's ratio. For the ice front of an Antarctic ice shelf, or for a tabular iceberg, we take $h = 200$ m. For solid glacier ice, $E \approx 8 \times 10^3$ MN/m^2, but for the lower density compacted snow in the upper part of the berg E is a good deal smaller. For a rough preliminary calculation, we shall take constant values of $E = 8 \times 10^3$ MN/m^2 and $E = 4 \times 10^3$ MN/m^2. For the unit weight of seawater we take the rounded value 10^{-2} MN/m^3, and for μ take 0.3. The resulting calculated values of L_* are 6.5 km for $E = 8 \times 10^3$ MN/m^2 and 5.5 km for $E = 4 \times 10^3$ MN/m^2. In broad terms, the critical wavelength for maximum stress is about 6 km. It should be mentioned that this is not necessarily a unique wavelength that creates maximum stress, since stress is proportional to wave amplitude. Nor is it necessary to identify breakage with the most severe combination of amplitude and wavelength, since in principle the ice could break at something less than the maximum stress that is attainable theoretically.

The critical wavelength produces "extreme fibre" stresses σ_*, where

$$\sigma_* = Ak(2/h)^{1/2}\,[E/3k(1-\mu^2)]^{1/4}. \qquad (11)$$

For $E = 8\times10^3$ MN/m², σ_* is $0.54A$ MN/m², and for $E = 4\times10^3$ MN/m² it is $0.38A$ MN/m², where A is in meters. Taking $\sigma_* \approx 0.54A$ MN/m², the stress would be 0.45 MN/m² for A = 1 m and 4.5 MN/m² for A = 10 m. The uniaxial tensile strength of ice under rapid loading is about 2 MN/m² for small intact laboratory specimens, but for large beams and slabs of freshwater ice tested in situ the apparent flexural strength is a good deal lower, say around 0.5 MN/m². Thus the critical wavelength would probably break the ice, almost irrespective of amplitude.

For icebergs smaller than 6 km across, the most dangerous wavelength for quasi-static loading is probably a wavelength equal to the width of the berg in the wave's direction of travel. Ignoring the fact that an isolated berg then behaves as a simple beam rather than as a continuous beam, application of the infinite plate theory gives a rough estimate of the stresses, with the error in the direction of underestimation. Following this procedure, it appears that for wave amplitudes up to 10 m and berg widths up to 2 km, the stresses are not necessarily destructive.

The dangerous wavelengths discussed so far have been those that maximize stresses according to a quasi-static analysis, but there is also a potential danger of resonance from waves of other frequencies.

To sum up, approximate calculations suggest that large tabular bergs with width to depth ratios in excess of 10 stand a good chance of being broken up by long wavelength ocean waves. These results are in general agreement with the observations on the size distribution of icebergs in or near the open ocean as contrasted with those in the pack ice as reported earlier in this paper and by Kovacs.[40] If there is any idea of towing large bergs, more detailed analysis of wave loading clearly takes high priority.

TOWING

Geophysical and engineering considerations

Towing through sea ice

Over much of the year, most Antarctic icebergs are found within the boundaries of the pack ice. This places restrictions on what icebergs can and cannot be towed at any given time, inasmuch as the power requirements for towing a large iceberg through heavy sea ice are enormous. For instance, if we take a representative thickness for Antarctic sea ice to be 1 m (in many places, thicknesses are greatly in excess of this value) and estimate the power required to move a 1-km-wide icebreaking ship through such ice at a velocity of roughly 0.5 m/s (1 knot) we obtain a value of 3.3×10^5 kW (445,500 SHP). It would take 17 of the largest tugs currently available (see section on *Tug power*) to provide this amount of power. In fact, the actual power requirements would be in excess of this value inasmuch as a blunt-ended iceberg is hardly as efficient an icebreaking system as a specially designed ship.

Because we can only tow icebergs that are either north of, or just on the edge of, the ice pack, it becomes critical to know where this highly mobile boundary is at any given time. This type of information is available from passive microwave images, which show the open ocean/pack ice boundary in the Southern Ocean quite clearly. A general discussion of the interpretation of this type of satellite image as applied to the polar regions can be found in reference 43. An idea of the possible changes in the location of the sea ice boundaries that can be expected during a year can be obtained from Figure 11 in reference 44 which shows the near-maximum and near-minimum boundaries for the Antarctic pack for 1973. A strategy for selecting an iceberg might be to monitor the general location of suitable icebergs found near the northern boundaries of the pack by the use of Landsat imagery. The tow could be started in the Austral summer or spring when the pack ice edge recedes to where the icebergs are located. After examination by geophysical methods, a compromise would have to be struck between selecting an iceberg at a location nearest to the delivery site and selecting one that has been protected from wave erosion by the presence of pack ice and does not contain detectable flaws.

Iceberg acceleration

It is of interest to know how long it will take to accelerate an iceberg up to its full towing speed, and how long it will take for the iceberg to stop after a tug ceases pulling.

Assume the tug has a maximum available bollard pull P that does not vary with speed over the range of towing speeds (say 0 to 1 knot). Further assume that the hydrodynamic resistance of the iceberg can be expressed as Cu^2, neglecting purely viscous effects in the initial stages of motion (there is no mathematical difficulty in including viscous effects, but computation is messier). The mass of the iceberg is M. The equation of motion thus becomes

$$P - Cu^2 = M\left(\frac{du}{dt}\right) \qquad (12)$$

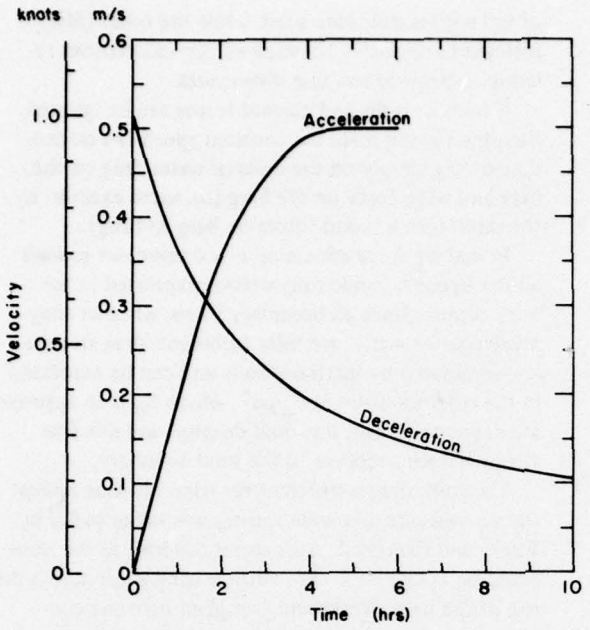

Figure 22. Acceleration and deceleration curves for an iceberg 1600×400×200 m assuming a form drag coefficient of 0.6, and that the towing force is that required to achieve a steady state towing velocity of ≈ 0.5 m/s (1 knot).

and a solution is readily obtained by separation of variables. The solution can be expressed in various ways ($\tan^{-1}$, $\tanh^{-1}$ or log), but we choose

$$t = (PC/M^2)^{-1/2} \tanh^{-1}\left[\frac{u(PC/M^2)^{1/2}}{P/M}\right] + A_1 \qquad (13)$$

where A_1 is an integration constant equal to zero when the iceberg starts from rest at time zero (when there is an initial velocity u_0, A_1 is just the $\tanh^{-1}$ term with u_0 substituted for u).

When the iceberg is traveling at velocity u and the tug suddenly ceases to pull, the equation of motion is simply

$$Cu^2 = -M\frac{du}{dt} \qquad (14)$$

for which a convenient solution is

$$t = \frac{M}{Cu} + A_2 \qquad (15)$$

where A_2 is an integration constant equal to $-M/Cu_0$ when u_0 is the velocity at time zero.

Figure 22 gives examples of the acceleration and deceleration of an iceberg that is 200 m thick, 400 m wide, and 1600 m long, assuming a form drag coefficient of 0.6, and taking P as the value required to achieve a steady-state towing velocity of 1 knot. In theory, it takes infinite time to reach 1 knot if the tug has no reserve of power, but in fact the velocity is within a few percent of the final velocity after about 5 hours. When the iceberg is cut loose at 1 knot, its speed drops to 0.2 knot in about 10 hours, and to 0.1 knot in about 22 hours.

Tensile towing stresses in the ice

If an iceberg is towed with cables attached to its "bow," longitudinal tensile stresses are developed by the skin-friction drag. The maximum stress is developed on a cross section immediately aft of the towing cable anchors, and it is approximately equal to the skin-friction drag divided by the section area. For typical dimensions and towing speeds, this stress is many orders of magnitude below the short-term tensile strength of icc, and at least three orders of magnitude smaller than the stress level at which creep becomes discernible. Even considering the low values of these stresses, it still may prove advantageous to couple with the iceberg via a net or a towing bridle that goes completely around the iceberg. Such a system would tend to contain the ice if the iceberg under tow splits into two or more pieces.

Melting of ice in transit

Melting of an iceberg by surrounding ocean water has always been recognized as a serious problem. Even at the low towing speeds that are envisaged, there is forced convection and effective heat exchange in the turbulent boundary layer. Because they could find no directly applicable experiments, Weeks and Campbell[1] used a correlation giving the average heat transfer coefficient for fully developed turbulent flow over a flat plate. Griffin[45] has now looked at this problem in some detail for the actual case of freshwater ice in seawater, obtaining melting rates similar to, but slightly higher than, the estimates of Weeks and Campbell. In actuality the situation is made additionally complex by the fact that melting shelf ice will release air bubbles which will stream along the sides of the iceberg. Also the melting process itself is likely to form a wavy ice surface, resulting in higher heat transfer rates.[46] Considering its import this is clearly a subject worthy of further investigation. Here we would like only to put forward a rough rule-of-thumb useful for making approximate estimates of the net amount of melting that might occur during a tow.

The rate of heat transfer to the iceberg surface increases with its velocity relative to the water in proportion to velocity raised to a power somewhat less than unity. The heat transfer rate tends to decrease with downstream distance along the boundary layer, being inversely proportional to distance raised to a power of approximately 0.15 to 0.2. The other big factor is water temperature, since the heat transfer rate is directly proportional to the temperature difference between the ice and the water. Therefore, a simple way to look at ice loss is to relate it to a summation of "degree-days" for the passage. The total ice loss at any stage of the journey (Z) can then be expressed as

$$Z = K\Delta \qquad (16)$$

where Δ is the mean water temperature summed for each day of the journey and K is a constant for a given towing speed and iceberg size. For a towing speed of 1 knot and an iceberg length of the order of 1 km, K is approximately 0.12 when Z is in meters and Δ is in Celsius degree-days.

With this simple estimating tool, it is easy to see the magnitude of melt losses, e.g. 100 days at an average water temperature of 10°C removes something of the order of 120 m from the outside of the iceberg. It is also easy to make the point that icebergs are unlikely to survive long journeys if melting goes unchecked, e.g. a 200-day passage at an average water temperature of 15°C would strip 360 m from the exposed surfaces of an iceberg that is only 200 m thick to start with.

Towing forces and energy requirements

We still have some uncertainties about how to calculate towing forces. The debatable components are 1) the Coriolis force, and 2) the gradient current force, both of which were included in the expression for constant-speed towing force by Weeks and Campbell.[1] The difficulty with the Coriolis force is that as the iceberg moves it creates a counterflow of an equal mass of water in the opposite direction. The displaced water should experience a Coriolis force that is of comparable magnitude to that acting on the berg, but in the opposite direction. There is probably effective coupling along the sides of the berg, but only weak shear coupling along the base. With regard to the current force, it would obviously exist if the berg were to be towed by winch from an anchor on the seabed, but if both berg and tug are being carried along by the same current (assuming negligible gradients in the horizontal and vertical directions) there is no effect on the towline force. There is, of course, a velocity vector produced by the gradient current. We both agree that current force can be neglected. As for the Coriolis force, one of us (*WW*) is still undecided, while the other (*MM*) is inclined to neglect it for exploratory calculations relating to bergs of towable dimensions.

If both Coriolis and current forces can be ignored, then the towing force for constant speed can be estimated very simply on the basis of water drag on the berg and wind force on the berg (or, more exactly, by the difference of wind forces on berg and tug).

In making force estimates, it is convenient to have all the hydrodynamic drag stresses expressed in the same terms. Since all boundary flows, whether they involve air or water, are fully turbulent, drag stresses are dominated by inertial effects and can be expressed in the common form $\frac{1}{2} C_d \rho u^2$, where C_d is an appropriate drag coefficient, ρ is fluid density, and u is free stream velocity relative to the solid boundary.

The form drag coefficient for wind blowing against the vertical side of a wide iceberg was taken as 0.6 by Weeks and Campbell. This seems too low, as the value could be as high as 2. For surface wind shear across the top of the berg, Weeks and Campbell used the conventional relation for turbulent boundary layers, in which the drag coefficient is expressed in terms of velocity gradient and roughness length. It is more convenient to take a direct value of C_d; for smooth snow surfaces this is about the same as the value for water flow in smooth channels, i.e. 2.5×10^{-3}.

The water drag and the air drag cannot be combined in a simple fashion. The total wind force on the berg will eventually create an equal and opposite water drag, with a corresponding drift velocity relative to the water. This can be completely independent of the action of the tug, and in any direction relative to the desired heading of the berg. The force applied by the tug will also eventually create an equal and opposite water drag force, with its characteristic velocity. Probably the simplest procedure is to treat the wind force and the towing force independently, combining the corresponding velocity vectors for the track calculations only.

There is a simple way to estimate the drift produced directly by the wind. The total drag created by wind F_a is

$$F_a = \frac{1}{2} [\rho_a u_a^2 (C_{dfa} A_{fa} + C_{dsa} A_{sa})] \qquad (17)$$

where ρ_a is air density, u_a is wind speed, C_{dfa} is the form drag coefficient for the iceberg side exposed to the wind, A_{fa} is the area of this side, C_{dsa} is the skin drag coefficient for the top of the berg, and A_{sa} is the area of the top. The reacting water drag F_w is given by an equation of identical form when the subscript a is replaced by subscript w to represent water properties and underwater

geometry. Thus the ratio of drift velocity u_w to the wind speed u_a is

$$\frac{u_w}{u_a} = \left[\frac{\rho_a}{\rho_w}\,\frac{C_{dfa}A_{fa} + C_{dsa}A_{sa}}{C_{dfw}A_{fw} + C_{dsw}A_{sw}}\right]^{1/2}. \qquad (18)$$

In this equation $\rho_a/\rho_w \approx 1.3\times10^{-3}$, $C_{dfa} \approx C_{dfw}$, $C_{dsa}/C_{dfa} = C_{dsw}/C_{dfw} \sim 10^{-3}$, $A_{fa}/A_{fw} \approx 0.2$ and $A_{sw}/A_{fw} = 0.2\,A_{sa}/A_{fa} \approx 1.2K$, where K is the ratio of length (or width) in the wind direction to the total thickness of the berg. With appropriate substitutions, the approximate value of eq 18 becomes

$$\frac{u_w}{u_a} = \left[1.3\times10^{-3}\times0.2\left(\frac{1+6K\times10^{-3}}{1+1.2K\times10^{-3}}\right)\right]^{1/2}. \qquad (19)$$

Unless K is quite large, the terms in K can be ignored, so that

$$u_w/u_a \approx 0.016. \qquad (20)$$

In other words, the drift speed of the berg relative to the surrounding water will be about 1.6% of the wind speed.

For the form drag of an iceberg in sea water, the values of C_d taken by Weeks and Campbell[1] were 0.9 and 0.4 for the initial and final stages of the tow respectively and 0.6 for an average value over the whole transit. These still seem to be reasonable estimates. In fact, if an iceberg is towed without protection we believe that the front end will ablate to a highly streamlined shape in a relatively short period of time.[47] The "final" C_d value of 0.4 is the result of the drag caused by the blunt "after-body" of the iceberg. For the skin-friction drag of ice in water, Weeks and Campbell used a relation giving C_d as a function of Reynolds number. For the specific value of Reynolds number that they suggested ($R_e = 2.8\times10^7$), $C_d = 2.5\times10^{-3}$. Actually this value of C_d can probably be used without further qualifications, as it is a good working value for the minimum value when water flows in very smooth channels. The exception here would be if the ablative process caused the ice/seawater interface to become physically rough.

The tug towing force at constant speed is primarily determined by the water drag which, as was the case for the wind drag, can be separated into form drag and skin-friction drag. The total drag force F_d is

$$F_d = \frac{1}{2}\rho_w u^2 (C_{df}A_f + C_{ds}A_s) \qquad (21)$$

where C_{df} is the form drag coefficient, A_f is the effective frontal area, C_{ds} is the skin drag coefficient, and A_s is the effective skin area. If the total thickness of the berg is T, the effective width and effective length can be expressed as $K_1 T$ and $K_2 T$ respectively, such that $A_f = K_1 T^2$ and $A_s \approx K_1 K_2 T^2 + 2(5/6)K_2 T^2$. Thus the total drag force can be expressed approximately as

$$F_d \approx \frac{1}{2}\rho_w u^2 C_{df} K_1 T^2 \left[1 + \frac{C_{ds}}{C_{df}}\frac{K_2}{K_1}(K_1 + 1.7)\right]. \qquad (22)$$

This indicates that form drag is likely to dominate for icebergs of manageable size and shape, since $C_{ds}/C_{df} \approx 3\times10^{-3}$. With $K_1 = 2$ and $K_2/K_1 = 4$, the skin drag term in the bracket is 0.044, i.e. skin drag amounts to less than 5% of the total drag.

For convenience in making numerical estimates, eq 22 can be written for a 200-m-thick berg as

$$F_d \approx 20.6\,u^2 K_1 C_{df}\left[1 + 3\times10^{-3}\frac{K_2}{K_1}(K_1 + 1.7)\right] \text{ MN} \qquad (23)$$

when u is in m/s. With realistic values of K_2/K_1 and modest values of K_1, the form drag alone probably gives a sufficiently close estimate:

$$F_D \approx 20.6\,u^2 K_1 C_{df} \quad \text{MN}. \qquad (24)$$

Thus for a 400-m-wide berg towed at 1 knot (0.5148 m/s) the form drag is approximately $10.92\,C_{df}$ MN, to which 5% or so can be added to allow for skin friction. With $C_{df} = 0.6$, $F_d \approx 6.9$ MN (1.55×10^6 lbf, or 773 tons). In general, the skin friction for a bluff iceberg can be accommodated by a factor close to unity. For preliminary estimates we can simply take

$$F_D \approx 22\,u^2 K_1 C_{df} \quad \text{MN} \qquad (25)$$

which makes a 7% allowance for skin friction.

The effective horsepower (EHP), or "towrope power," is simply the total drag force multiplied by the towing speed, i.e.

$$P_t = F_d u \qquad (26)$$

where P_t is the towrope power or EHP. In other words, the foregoing expressions for towing force give the corresponding power when u^3 is substituted for u^2. For conventional ships, the towrope power divided by the

power of the propeller shaft (SHP) is known as the propulsive coefficient. For single screw cargo ships, the propulsive coefficient (EHP/SHP) might be in the range 0.65 to 0.85. This probably implies that the shaft power of an iceberg tug will have to be somewhat greater than its towrope power.

Referring back to the example of towing force that was just given (6.9 MN or 1.55×10^6 lbf), the corresponding towrope power (EHP) is 3.55 MW or 4760 hp at a speed of 1 knot. This is a very modest power level *if efficient propulsion can be arranged.*

For some purposes it may be convenient to express the force, power and energy in relation to the frontal area, volume and mass of ice that is being moved. The towing resistance can be expressed approximately in terms of the form drag, with skin friction taken into account by a factor β:

$$F_d \approx \frac{1}{2} \rho_w u^2 C_{df} A_f \beta \tag{27}$$

where β is slightly greater than unity. If the tabular iceberg is approximately rectangular in plan, with volume V, mass M, and length L, then

$$\frac{F_d}{A_f} \approx \frac{1}{2} \rho_w u^2 C_{df} \beta \tag{28}$$

$$\frac{F_d}{V} \approx \frac{\rho_w u^2 C_{df} \beta}{2L} \tag{29}$$

and

$$\frac{F_d}{M} \approx \frac{\rho_w}{\bar{\rho}_i} \frac{u^2 C_{df} \beta}{2L} \tag{30}$$

where $\bar{\rho}_i$ is mean ice density as given by eq 4.

The corresponding expressions for specific power can be obtained by substituting u^3 for u^2 in eq 28, 29 and 30.

Putting some numbers into these relations, we note first of all that for 1 knot towing speed the stagnation pressure ($\frac{1}{2} \rho_w u^2$) is 136 N/m^2, or 0.0197 lbf/in.^{2}. Thus F_d/A_f might be about 65% of the stagnation pressure for $C_{df} \approx 0.6$.

The expression for F_d/V can be used to obtain an estimate of the specific energy for towing E_{st}, to move the iceberg a distance equal to its own length:

$$E_{st} = \frac{1}{2} \rho_w u^2 C_{df} \beta. \tag{31}$$

In numerical terms, E_{st} for traveling $1000L$ at 1 knot is $C_{df} \beta \times 136$ kN/m^2 (= kJ/m^3) or $C_{df} \beta \times 19.7$ lbf/in.^{2} (= in.-lbf/in.^{3}). These are very modest values for such a long journey, which amounts to 1600 km or 1000 miles for an iceberg 1.6 km long. By comparison, the specific energy for melting ice is 306 MN/m^2 or 4.4×10^4 lbf/in.^{2}, i.e. it takes more than 2000 times as much energy to melt an iceberg as it does to tow it efficiently for 1000 miles. The specific energy for lifting ice through a height of 1 m is 8.92 kN/m^2, so that a 1000-mile (1600-km) tow takes as much energy as a lift of 15 m.

The towing force per unit mass, given by eq 26, is an acceleration that can be compared with the gravitational acceleration, which gives the lifting force per unit mass. For towing at 1 knot, F_d/M for an iceberg 1.6 km long is $10^{-4} C_{df} \beta$ m/s^2, or about five orders of magnitude smaller than g.

Tug characteristics

Tug power

The size and power of individual tugs is still increasing. A decade ago, the power limit was represented by the 9000-hp *Zwarte Zee* of Smit International. At the time of the Weeks and Campbell iceberg study in 1973, the limit was represented by the 20,000-hp *Oceanic* of Bugsier-Reederei & Bergungs. At present, the 26,200-hp tugs *S.A. Wolraad Woltemade* and *S.A. John Ross* of the South African Marine Corporation seem to set the limit.

Figure 23 gives a plot of installed power against displacement tonnage for a wide range of existing tugs. Lines are drawn on the plot to represent different levels of specific power. Some oceangoing tugs have up to 45 hp/ton (37 kW/tonne), although the most powerful tugs have approximately 10 hp/ton (8.2 kW/tonne). These values are in terms of installed horsepower rather than shaft horsepower because the information was readily available in that form. The ratio of shaft horsepower to installed horsepower is typically about 0.97 for geared drive and about 0.79 for electric drive. The specific power of tugs is comparable to that of high-speed surface ships such as destroyers. However, the propulsion requirements are quite different.

If a tug were to be built specially for independent operation over long periods, it would probably have a comparatively low power/weight ratio because of the need to carry fuel and supplies.

Towing capabilities of tugs

The towing force of a tug is determined largely by the shaft horsepower and the propeller characteristics, and it is calculable when these things are known. However, in Figure 24 we have chosen to plot values of rated bollard pull for existing tugs as a function of installed

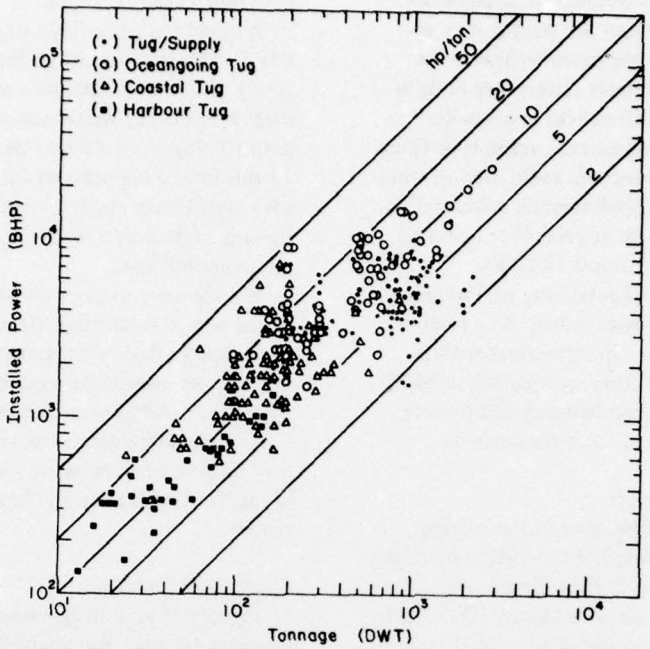

Figure 23. Plot of installed power versus displacement tonnage for a wide range of existing tugs.

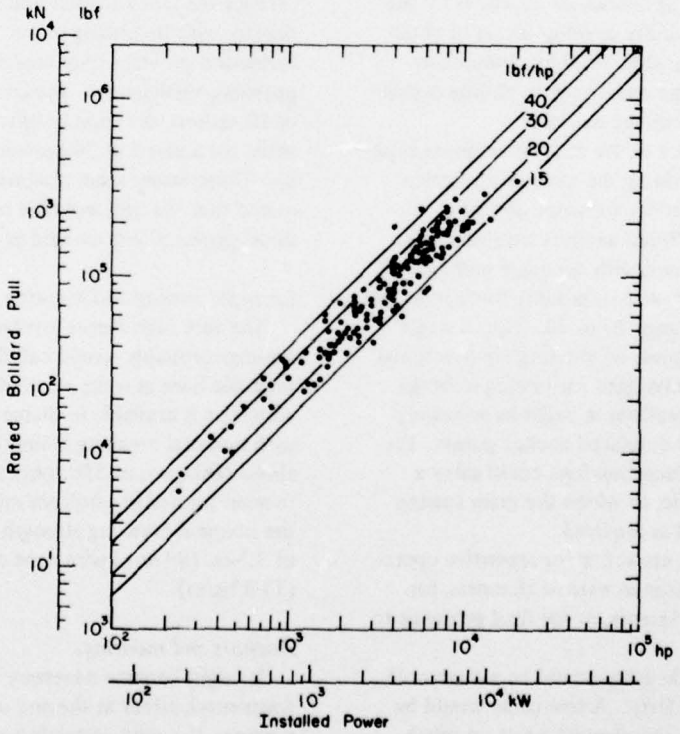

Figure 24. Rated bollard pull versus installed power for a wide range of existing tugs.

power to give an impression of practical capabilities. The data are taken largely from the results of an industry survey published by the journal *Offshore* in March 1977. The scatter reflects differences of drive systems (geared, electric), differences in propeller systems (open, shrouded), differences in vessel type (pure tug, tug/supply), and differences in evaluation of what represents a realistic bollard pull (tested, calculated, or guessed). Most of the data lie in a band representing pulls of 17 to 30 lbf/hp (0.10 to 0.18 N/W).

It is probably safe to extrapolate tug performance on the basis of these pull/power ratios. An earlier deduction that the pull/power ratio decreases with increasing power was derived from an equation in which two of the variables (propeller diameter and power) are actually implicitly related for real situations.

Towing capabilities of winches

In principle, bergs could be towed by winching cables against seabed anchors, and the technique might be practicable in reasonably shallow water. The mechanical efficiency of a winch is almost 100%, and very high forces can be developed with modest power at the towing speeds that are envisaged. At 1 knot, the pull/power ratio is about 1.94 N/W (326 lbf/hp), which is roughly 10 times greater than the best pull/power ratios for screw driven tugs.

Winches used for laying submarine pipelines by the bottom-pull method typically develop forces of about 150 tonnes (which means that 1000 hp could be developed at 1 knot). Single winches with pulling capacities in excess of 200 tonnes are available.

A standard ship anchor of the drag-embedment type might be capable of providing the necessary reaction when properly set with adequate scope and/or a weighted leader chain. Burial anchors weighing up to 45 tonnes are available, and with adequate embedment in bottom sediments the ratio of holding force to anchor weight might be in the range 20 to 30. Thus a single anchor is potentially capable of resisting unidirectional pulls of the magnitude envisaged for towing icebergs. On some kinds of rock seafloor it might be necessary to consider permanently emplaced anchor points. Preset or premanently emplaced anchors could carry a short buoyed leader cable, to which the main towing cable would be shackled as required.

Winch tows might be attractive for repetitive operations, for precise navigation in narrow channels, for negotiation of adverse currents, or for final guidance to the terminal mooring.

An exotic variant of kedging would be a mammoth version of the old chain ferry. A tow cable would be laid on the seabed along the planned route, in much the same way as telephone cables are laid. The berg would be hauled along the cable by means of capstans.

Fuel requirements for tugs

A diesel tug with direct or geared drive might have a fuel consumption rate of about 0.4 lb/SHP-hr (67.5 g/MJ). In other words, for each 10,000 SHP (7500 shaft kW) the tug would use about 2 tons of fuel per hour (0.5 kg/s), or 48 tons per day (44 tonnes/day). At this rate, a tug utilizing 20,000 SHP (14,900 shaft kW) would burn about 17,500 tons (15,900 tonnes) of fuel on a 6-month tow, or 26,300 tons (23,800 tonnes) on a 9-month tow.

If a tug were to carry its own fuel for a complete round trip to Antarctica, its displacement might have to be double that of a conventional tug, and some additional power would be required to compensate for the bigger hull. It has been suggested that a converted tanker should be used as an iceberg tug, but this idea may have some drawbacks. Alternatives include rendezvous with a supply ship, or escort by a tanker/tender.

Capital value of tugs

Figures 25 and 26 give some data on owners' valuations for existing and newbuilding tugs. Assessed value is plotted against tonnage, and against installed power, with the expectation that the upper limit envelope might reflect current costs for new vessels. Data were also plotted as $/hp versus hp/ton (not shown), indicating a tendency for the unit cost of power to decline slightly with increasing power to weight ratio. This information provides only crude indicators, but it is probably sufficient for present purposes. For a vessel of 10 hp/ton, the capital value might be about $800/hp, while for a vessel of 20 hp/ton it might be about $600/hp. These values seem reasonable, as it has been estimated that the unit installed cost for large stationary diesel power plants on land is as much as $550/hp.

Lines for towing and mooring

The very high forces involved in towing and mooring icebergs probably would call for use of the strongest available lines at some stage of the project. High strength wire rope is available in diameters up to 3.5 in. (89 mm), with nominal breaking strength at this maximum size about 600 tons, or 550 tonnes. The maximum working tension for design purposes might be about one-third the nominal breaking strength. The unit weight (in air) of 3.5-in. (89-mm) wire rope can be taken as 22.7 lb/ft (33.8 kg/m).

Anchors and moorings

It might become necessary to anchor the iceberg (or fragments), either at the end of the journey or in mid-passage. It would certainly be necessary to have a secure mooring system at the terminal where processing is undertaken.

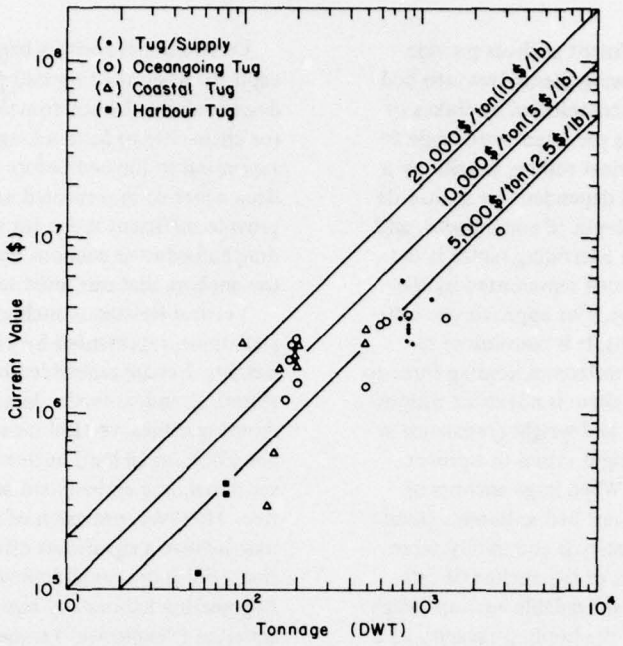

Figure 25. Assessed value of existing tugs plotted against tonnage.

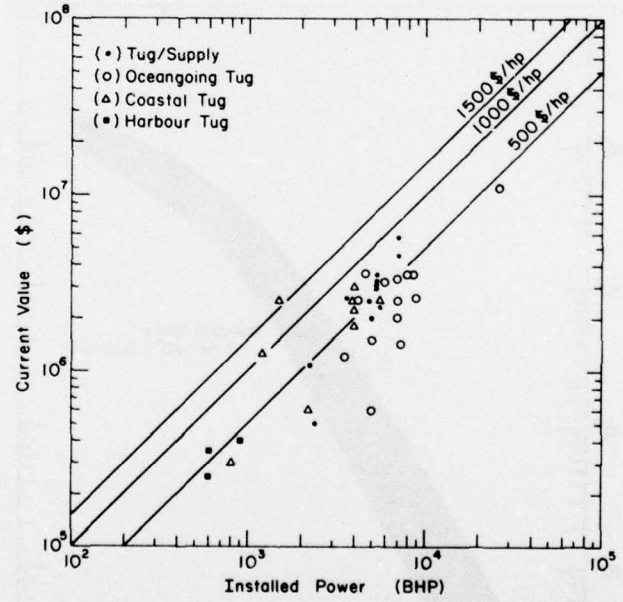

Figure 26. Assessed value of existing tugs plotted against installed power.

Conventional drag embedment anchors provide horizontal resistance by plowing themselves into bed sediments. The digging is accomplished by flukes of some kind, which are set at a predetermined angle to the shank, and stabilized against rolling, usually by a transverse bar. Resistance is dependent on anchor design, properties of the bed, depth of embedment, and length of drag. However, an overriding factor is the size of the anchor, which is well represented by the weight for a particular design. For approximate estimates of anchor requirements, it is convenient to think in terms of a ratio of horizontal holding force to anchor weight, even though there is not exact proportionality between resistance and weight (resistance is typically proportional to weight raised to a power somewhat less than unity). When large anchors of modern design are set in typical bed sediments (mud, clay, sand), the holding capacity is commonly more than 10 times the dry weight of the anchor (it can exceed 30 times). The largest available anchors weigh 50 tons (45 tonnes), so that the holding capacity of a single anchor can well exceed 500 tons (450 tonnes), which is comparable to the breaking strength for a single cable of the largest diameter wire rope.

Conventional anchors begin to lose their holding capacity when the imposed pull is more than a few degrees above the horizontal, so that an anchor cable (or chain) has to form a long catenary that becomes tangential to the bed before it reaches the anchor. In deep water or in restricted areas it may be difficult to provide sufficient scope for spread moorings that use drag embedment anchors, and it becomes desirable to use anchors that can resist vertical force components.

Vertical resistance anchors are more permanent installations, represented by piles, plates, screws or deadweights that are embedded by drilling, driving, jetting, vibrating, and so forth. In addition to permitting shorter mooring cables, vertical resistance anchors can provide good holding in hard bottom sediments, where conventional drag embedment anchors are not very effective. However, provision of a vertical resistance anchor may involve a significant effort in underwater construction. For more rapid deployment, the U.S. Navy Civil Engineering Laboratory has developed propellant-actuated ("explosive") embedment anchors that have nominal rated holding capacities of 5, 10 and 50 tons.

For the iceberg terminal it would probably be necessary to have a specially designed multi-point mooring

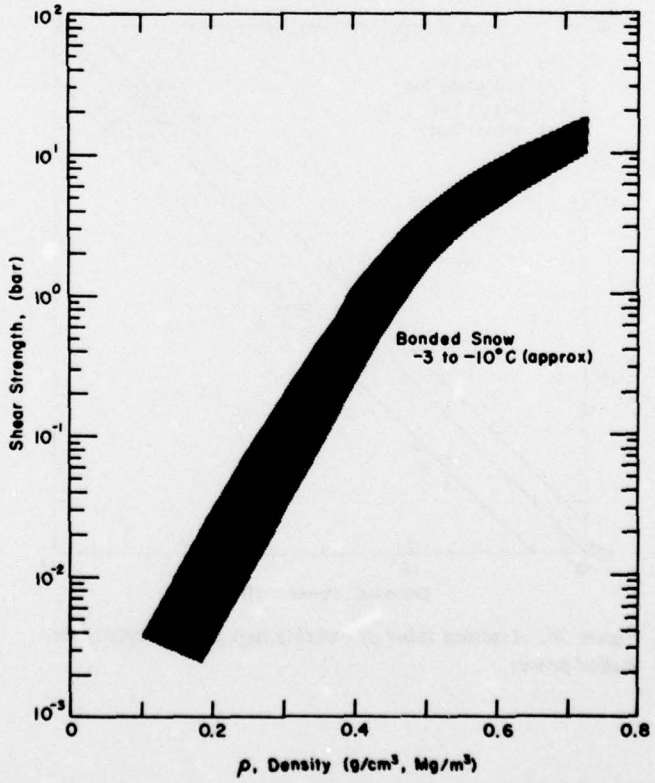

Figure 27. Shear strength of bonded snow versus density.

system installed either prior to arrival of the berg, or immediately upon arrival.

Cable anchorages in snow and ice

There has been concern about the problem of installing bollards or anchors to provide towing points on the iceberg. Concern is well founded if conventional bollards are envisaged, but subsurface anchorages of the deadman type avoid most of the difficulties of radiation absorption, heat conduction, and preferred meltwater infiltration. A deadman structure could be installed at right angles to the tow direction, either in a cut-and-cover trench or in a small tunnel. The tow cables or bridles could be carried to the "bow" of the iceberg through slots or boreholes.

The shear strength of dry snow and ice at temperatures between $-3°$ and $-10°C$ is indicated in Figure 27. These values are for low levels of normal stress or bulk stress. For "warm" snow and ice that is subject to an appreciable overburden pressure, the lower limit of the data band can probably be taken for preliminary design estimates.

The nominal breaking strength of the largest wire rope is about 500 tonnes. A buried deadman anchor would be set in snow of at least 0.5 Mg/m^3, and the strength of the snow in a potential failure plane would be of the order of 1 bar. Thus the required area for a potential shear plane would be of the order of 50 m^2 if it had to match the maximum pull of a single cable that breaks at 500 tonnes. For a deadman buried 5 m below the surface, the required width would be only about 5 m if the potential shear plane is inclined at 30° to the horizontal. Without going into detailed analysis, it seems likely that conservatively designed anchors can be provided without much trouble.

HANDLING AND PROCESSING

Cutting and boring with thermal devices

Various kinds of thermal devices have been used to cut and drill in ice and ice-bonded soils. They include steam points and steam bars, hot water melters, supersonic flame jets, lasers, and electric heaters. All are handicapped by the inherently high specific energy consumption that results from the high heat of fusion of ice. Complete melting of solid ice from an initial temperature of $-5°C$ calls for 316 MJ/m^3 even with perfect thermal efficiency. By contrast, efficient mechanical devices can cut ice with specific consumptions less than 1 MJ/m^3. On the other hand, while thermal devices require considerable energy, they do not require that much *force* be transmitted, and this is an asset where deep penetrations are required.

The power requirements for thermal penetration can be expressed conveniently in terms of surface energy flux or power density Q_p, i.e. power per unit area of the penetrator. The *minimum* required power density for penetration at velocity v_p is determined by the rate at which sensible heat and latent heat have to be supplied:

$$Q_p = \rho_i v_p (c_i \Delta\theta + L_i) \qquad (32)$$

where ρ_i is density (≈ 0.89 Mg/m^3 for bubbly ice), c_i is apparent specific heat (2.12 J/g-K for pure ice), L_i is the latent heat of fusion (333.5 J/g for pure ice at 0°C and atmospheric pressure), and $\Delta\theta$ is the difference between initial ice temperature and the melting temperature. Q_p is shown as a function of v_p and $\Delta\theta$ in Figure 28. Actually, the sensible heat is not very significant, and for present purposes it is sufficient to express Q_p as

$$Q_p = 0.3 v_p \quad MW/m^2 \qquad (33)$$

where v_p is penetration rate in mm/s.

Values of Q_p given by eq 32 and 33 take no account of thermal efficiency. Operational experience with various types of thermal borers indicates that melting efficiency at the penetrator is about 50%, so that a more practical estimate of required power density is obtained by introducing a factor of 2 into eq 33, i.e.

$$Q_p = 0.6 v_p \quad MW/m^2 \qquad (34)$$

when v_p is in mm/s. It might be noted that the 50% melting efficiency does not cover line losses and energy conversion losses.

Penetration with electrothermal devices

For deep penetration, electrothermal equipment seems more attractive than other thermal devices. A practical estimate for the power density of an electrical resistance heater can be obtained from eq 32 for any given penetration rate. However, there are limits to the power density that is practically useful. First of all, service life is inversely related to power density, since higher temperatures are involved (with extreme power density, the heater would pop like a flash bulb). Secondly, there are heat transfer complications when very high power densities are applied, since boiling sets in at a critical temperature, and vapor bubbles block heat transfer. For a service life of 1000 hours or better, maximum power densities of electric heaters are about 1 to 3 MW/m^2 with existing technology. This limiting range is almost identical to the maximum power densities achieved with the Los Alamos "Subterrenes" designed for melt penetration of rocks.

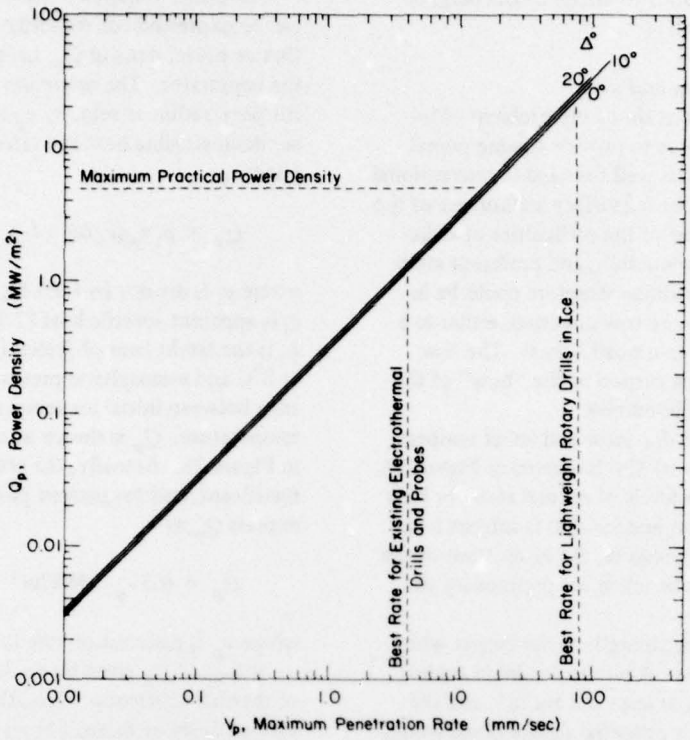

Figure 28. Power density versus maximum penetration rate for thermal coring or cutting. Here Δ° is the difference between the initial ice temperature and the melting temperature.

Taking 3 MW/m² as a maximum practical power density, a working estimate of maximum feasible penetration rate is obtained from eq 33:

$$(v_p)_{max} = 3/0.6 = 5 \text{ mm/s}. \qquad (35)$$

The best operational rate obtained so far with electrothermal drills is about 4 mm/s.

To estimate the power needed to service an electrothermal device, it is necessary to account for line losses and energy conversion losses. With local power generation the line losses could be kept very small, and with a direct-coupled diesel-electric generating set there are only small electrical or mechanical transmission losses. Thus most of the loss is represented by conversion of fuel oil to mechanical energy, and in round terms this can be accounted for by increasing the electrical power requirement by a factor of 3 (i.e. 33% conversion efficiency). A working estimate of required generator input power for on-site generation is therefore obtained from eq 34 as

$$(Q_p)_{input} = 3Q_p = 1.8v_p \quad \text{MW/m}^2. \qquad (36)$$

Without going into any further details, we shall assume that thermal drills have rather little to offer in iceberg towing and processing, since rotary drills are very much more efficient for general purpose drilling.

Electrothermal cutting

Electrothermal knives have been proposed for shaping the iceberg in preparation for towing, and for slicing up the iceberg for processing at a shallow water terminal. Because of the very high specific energy and high power density, there is a strong incentive to make the thermal knife as thin as possible, and to settle for the lowest usable penetration rate.

The thickness of a linear penetrator depends to some extent on whether it is to have any sort of rigidity, or whether it is to be a flexible wire or foil. The minimum thickness might be of the order of 1 mm for a practical device, and 10 mm would certainly be close to the maximum thickness that could be considered for large scale work.

To penetrate the complete thickness of a somewhat depleted berg 170 m thick, the required rate would be about 2 mm/s for penetration in one full day, or 0.2

mm/s for penetration in 10 days of continuous operation. Assuming an edge thickness of 1 mm, and a cut length of 100 m, the penetrator area is 0.1 m^2. The required power density from eq 34 is 1.2 MW/m^2 for penetration in 1 day, or 0.12 MW/m^2 for penetration in 10 days. With an area of 0.1 m^2, the electrical power requirements are 0.12 and 0.012 MW for penetration in 1 and 10 days respectively. The corresponding engine power requirements for on-site generation are about 360 and 36 kW (480 and 48 hp) respectively. If the edge thickness were to be 10 mm instead of 1 mm, then these power requirements would increase by a factor of 10.

Making vertical cuts by pre-split blasting

One way to make vertical cuts in the iceberg is to use explosive pre-shearing, or pre-splitting. The relevant blasting technology has been reviewed and applied to ice elsewhere, and a small scale operation has been carried out in Antarctica.[48 49]

The general idea is to drill a line of vertical holes, and pressurize them with decoupled explosive charges, thus propagating cracks which join up to form a split along the line of holes. The required ratio of hole spacing L to hole diameter D is approximately 10. Decoupling is achieved by suspending a column charge of diameter d inside a hole of diameter D, and the ratio D/d is termed the decoupling ratio. For ice, $D/d = 5$ should give satisfactory results. With this ratio, the required weight of explosive per unit column length w is given by

$$w = 7.85\times10^{-4}\, G_s d^2 = 3.14\times10^{-5}\, G_s D^2 \quad \text{kg/m} \qquad (37)$$

where d and D are in mm, and G_s is the specific gravity of the explosive. With $L/D = 10$, the charge weight per unit cut area F_{ps} (the pre-shear factor) is

$$F_{ps} = w/L = 0.314 G_s L \quad \text{kg/m}^2 \qquad (38)$$

where L is in m. There are some other details, such as required "collar distance," which need not be gone into here.

Examination of eq 38 reveals an optimizing problem for a practical operation. As hole spacing L increases, the explosive consumption per unit cut area increases. Furthermore, because L/D is constant, the required hole diameter increases as L increases, necessitating heavier duty drilling equipment. However, the required number of holes decreases as L increases.

For a practical operation the range of choice for hole diameter D, and therefore for L, is quite small. Minimum practical values are around D = 100 mm, L = 1 m. Maximum convenient values might be around D = 150 mm, L = 1.5 m. For a 100-m-long cut through a 170-m thickness of ice, the lower values of D and L demand 100 holes, each 170 m deep, and an explosive consumption of 6940 kg (3150 lb) if G_s = 1.3. With the higher values of D and L, about 67 holes are required, each 170 m deep, and the explosive consumption is about 10,400 kg (4722 lb).

Primary fragmentation by blasting

As a preliminary to the preparation of ice for delivery, blasting could be employed for primary fragmentation. There are two broad approaches: bench blasting and crater blasting.

Bench blasting is the standard industrial procedure used in quarries, open-pit mines, and surface excavations. Shotholes are drilled, either vertically or with slight inclination, in one or more lines that run parallel to a more or less vertical face, or bench. Modern practice favors use of large diameter shotholes loaded with relatively inexpensive explosives or blasting agents having a nitro-carbo-nitrate or ammonium nitrate base. Blasting procedures are optimized so as to minimize cost, taking into account drilling costs, explosive costs, and required production rate. Relevant parameters include bench height, hole diameter, explosive load, hole spacing (in a line parallel to the face), and burden (distance from hole to free face, or distance between parallel lines of charges).

Bench blasting tests were made[50 51] on massive ice in a study of explosive demolition of arctic "ice islands," which are actually small tabular bergs. It was found that ice is somewhat easier to blast than typical rocks, but not much so. There were some indications that yields might be enhanced in cold friable ice, but under springtime conditions the best yield was 2.2 m^3/kg (i.e. volume of ice broken per unit weight of explosive). This was obtained with a bench height of 7.3 m, spacing and burden of 3.7 m, hole diameter of 86 mm, and loading of 45 kg per hole. The explosive was an aluminized ammonium nitrate slurry sensitized with TNT and primed with TNT/PETN.

Crater blasting is used mostly in military engineering, although multi-crater modifications are used in civil works for mining and tunneling, trenching, and sinking cuts. In the simple form, a compact charge is set below the surface of a semi-infinite medium at the base of a well-stemmed drill hole. A roughly conical crater is formed, its dimensions being determined mainly by material type, charge size, and charge depth. Two craters have to be distinguished: the apparent crater, which is the open hole left by the explosion, and the true crater, which embraces the complete broken zone.

The true crater, whose limits are usually concealed by debris, is the one that is of interest here.

Cratering tests have been made in glacier ice[52] and relevant parameters determined (radius, depth and volume of true and apparent craters; optimum and critical charge depths). A representative value for the best attainable yield was about 4 m^3/kg. Without digressing into a discussion of scaling, it is difficult to give much information on linear dimensions of craters. However, if linear dimensions are scaled with respect to the radius r for an equivalent spherical charge of specific gravity 1.3, distances can be given in dimensionless form as multiples of r. Using this convention, the optimum charge depth, which maximizes radius and yield, is 25 ± 3.5. The corresponding radius for the true crater is 28 ± 7.

On the available evidence, crater blasting in ice is much more efficient than bench blasting in energetic terms, and it is much more economical of drilling effort. Bench blasting gives more uniform and controllable fragmentation, and it tends to be a more orderly procedure.

Primary fragmentation by mechanical sawing

An ice surface can be excavated and broken into large fragments by "rib-and-kerf" sawing. Parallel saw cuts are made perpendicular to the surface, leaving ribs of ice between the cuts. These ribs are cantilever slabs; when flexed, they break at the encastré end if the proportions are suitable. Indications are that such ribs can easily be snapped off at the base if the ratio of rib height to rib thickness is 1.5 to 2.

Relatively deep sawcuts can be made with large chain saws of the kind used for mining coal, potash, and other soft minerals. Without developing new equipment, cuts up to 8 m deep could be made. The kerf (cut) width for typical equipment is about 170 mm. Maximum useful power density for such equipment is about 0.6 MW/m^2 (cutter power divided by cutting area). Specific energy consumption depends a good deal on how well the equipment has been adapted. For instance, an unmodified coal saw cutting glacier ice gave a specific energy consumption of 12 MJ/m^3, which is an order of magnitude higher than what ought to be attainable with skillful design. The best recorded performance with a slightly modified coal saw is 2.8 MJ/m^3.

A simple estimate of traverse speed U can be made from the specific energy consumption E_s and the power density Q_p:

$$U = Q_p/E_s \sin\phi \qquad (39)$$

where ϕ is the bar angle of the saw. Taking $\phi = 90°$ (bar perpendicular to the surface), $Q_p = 0.5$ MW/m^2, and $E_s = 3$ MJ/m^3,

$$U = 0.5/3 = 0.17 \text{ m/s}. \qquad (40)$$

If cuts are made to a depth of 8 m with a spacing of 4 m, ice can be prepared for primary fragmentation at a rate of 5.44 m^3/s, or almost 20,000 m^3/hr. The input power for this production rate, excluding conversion losses, would be about 680 kW (912 hp). This kind of power level is perfectly feasible for a single independently powered machine. It should be noted, however, that careful design is required to attain specific energy consumptions of the assumed magnitude.

Final breakout of sawed ribs calls for a second tool to flex the ribs. This could be a bulldozer blade, a rolling wedge, or a hydraulic splitter.

Comminuting ice with machines

Mechanical comminution of the ice could involve secondary crushing of large fragments produced by a primary process, or it could be a continuous mining process employing cutting machines.

Rock crushers of the kind used in quarrying and mining are efficient machines. A rough estimate of specific energy consumption can be obtained by taking it as $\sigma_c \times 10^{-3}$, where σ_c is the uniaxial compressive strength of the material being crushed (specific energy has the dimensions of stress, and there is a rationale for normalizing specific energy with respect to the strength of the material being worked). Taking σ_c for rapidly loaded ice as 10 MN/m^2, the specific energy for crushing would be of the order of 0.01 MJ/m^3. This is an extremely favorable value, but of course it only covers *secondary* breakage. Restating the specific energy in terms of power and production rate, a good crusher ought to be able to process 1 m^3/s for each 10 kW of power.

An alternative to two-stage processing is a method whereby ice is cut directly from the mass by mining or excavating machines that produce chips suitable for delivery to conveyors or slurry pipelines. Typical mining and excavating machines, being designed for work in relatively hard rock, produce very small cuttings or chips. This is inefficient in energetic terms, since specific energy consumption is inversely related to the specific surface area of the comminuted material. It can also be very troublesome in ice, since fine fragments are surface-active and have a tendency to adhere (creating difficulties with conveying systems). However, a great deal of experimental and theoretical work has been

done on machine design for special-purpose excavators, and there should be no great difficulty in adapting existing machines for ice-processing.

The most practical approach is to take an existing machine of suitable morphology, say a continuous miner of some kind, and modify tool geometry, tool layout, head speed, and traverse speed to obtain large chips and low specific energy when working in ice. A realistic design goal is a specific energy consumption of 1 MJ/m^3 or less. This implies that a properly designed machine could process ice at a rate of at least 0.1 m^3/s for 100 kW of cutter power. This kind of production rate has been achieved with experimental machines. However, experience has shown that "seat-of-the-pants" designs and modifications can produce doleful results.

Slurry pipelines

Comminuted solids can be transported in pipelines as suspensions or slurries. Coal can be transported economically as a water slurry, and slurry transport for ice may be even more attractive, since the solid phase is almost neutrally buoyant. Snow-water slurries have been studied, but in cold environments they have proved troublesome because of the tendency for fine ice particles to adhere, and also because the water and the snow slush tend to separate. However, with coarse chips and warm surroundings this is not likely to be a problem.

One question is how much water is needed to slurry ice chips. A mass of coarse and fairly uniform ice chips is likely to have an effective porosity of about 0.45. To completely fill the accessible pores with water, the added water has to amount to about 80% of the ice volume or about 90% of the ice weight. Snow/water slurries are quite fluid at a 50/50 mixture by weight, and similar proportions might be appropriate for transporting ice. We have not yet looked into the pumping requirements, but would not expect flow resistance to be much more than that for water alone, especially as the ice/water ratio will decrease with distance traveled.

We would estimate that the slurry could travel in fairly large pipes at velocities up to about 3 m/s, so that a pipe of about 1 m diameter could deliver at the rate of about 2.4 m^3/s, or about 0.2 million cubic meters per day.

Data for transport of rocks and coal suggest that moderately high concentrations of ice could be pumped for specific energy expenditures of less than 13 MJ/m^3 for a 1-km transport distance. This specific energy, which is based on the volume of the solid fraction, is equivalent to 6 kW-hr/ton-mile.

CONCLUSION

In this paper we have tried to cover a wide range of relevant topics in the hope of giving a balanced picture of the technical problems involved in transporting and processing icebergs for water supply. The treatment of each topic is necessarily brief and simple, but probably adequate to illustrate the kind of trade-offs that would have to be made. While our primary intention is to provide information without adopting an advocacy position, certain conclusions seem unavoidable. Some of these have been reached earlier by others, yet they bear repeating.

a. No unprotected iceberg, no matter how long or wide, would be likely to survive the ablation caused by a long trip to low latitudes. To be more specific, if Δ in eq 16 becomes larger than roughly 1700, the solid assets under tow will have totally liquefied. On shorter journeys, such as to Australia, unprotected tows may still be possible. (Assuming a path length of 3000 km and an average speed of 0.5 m/s (1 knot) the travel time is approximately 70 days. Because the average water temperature is $\approx 5°C$, corresponding to a temperature difference relative to ice melting in sea water of $\approx 7°C$, the estimated melt loss is roughly 60 m of ice.)

b. Icebergs that have a horizontal dimension exceeding about 2 km may well be prone to mechanical break-up by long wavelength swells. Thinning by ablation would make this problem worse, as would the presence of crevasses, in that both reduce the effective thickness of the iceberg. Although the problem is treated only approximately here, the results seem credible because they appear to be in agreement with the limited observational data on real iceberg sizes.

c. To avoid the dangers associated with an iceberg capsizing, the width of a 200-m-thick iceberg should always be more than 300 m. Cliff erosion and vertical thinning are factors to be considered in assessing long-term stability.

d. For towing efficiency, the length to width ratio of a towed iceberg should be appreciably greater than unity.

e. For any sort of a pilot project, the selected iceberg would have to be quite small, if for no other reason than the practical availability of tug power (it is unreasonable to postulate development of a super-tug for a pilot project).

Putting all these considerations together, it seems that there may be little choice in the size iceberg that is suitable for towing. The iceberg cannot be much more than 2 km long and 0.5 to 2 km etc. wide, depending upon what length to width ratio is judged to

be most advantageous. These dimensions correspond to 0.2 to 0.8 km^3 of ice respectively or roughly 0.12 to 0.52 km^3 of ice delivered off the coast of Australia. Would the delivery of such quantities of ice to Australia be a viable operation? We have not worked through a complete scenario, but would guess that it might be viable only if the water was intended for industrial and municipal uses.

In his keynote address at the First International Conference on Iceberg Utilization Henri Bader accused Weeks and Campbell[1] of being expansionists, a criticism that is well taken. However, the Weeks and Campbell paper made no pretense of being a realistic engineering study. In the present paper we have considered some of the geophysical and engineering aspects of the problem in more detail, with the result that we have had to shrink the scale of the geophysically possible to where it may nearly coincide with what is practically feasible. This is useful in that it provides focus and suggests where the idea of iceberg water might go from here. If the idea is feasible, it would appear to be most feasible for southern Australia. The resulting operation would provide the experience necessary to assess realistically the chances of successful delivery of icebergs to more distant sites, and the time to contemplate ways of solving the formidable problem of decreasing in-transit melting losses by isolating icebergs from the surrounding ocean.

LITERATURE CITED

1. Weeks, W.F. and W.J. Campbell (1973) Icebergs as a fresh water source: an appraisal. *Journal of Glaciology*, vol. 12, p. 207-33.
2. Hult, J.L. and N.C. Ostrander (1973) Antarctic icebergs as a global fresh water resource. Rand Report R-1255-NSF, 83 p.
3. Al Faisal, M. (1977) New water resources for desert development from icebergs. In *Alternative strategies for desert development and management.* UNITER/State of California, Sacramento.
4. Hult, J.L. (1977) Water supply from imported Antarctic icebergs: a pilot program. In *Alternative strategies for desert development and management.* UNITER/State of California Conference, Sacramento.
5. Swithinbank, C. and J.H. Zumberge (1965) The ice shelves. In *Antarctica* (T. Hatherton, Ed.), Methuen and Co., Ltd., p. 199-220.
6. Crary, A.P., Personal communication.
7. Budd, W., I.L. Smith and E. Wishart (1967) The Amery Ice Shelf. In *Physics of snow and ice* (H. Oura, Ed.). *Proceedings of the International Conference on Low Temperature Science*, Hokkaido University, Sapporo, vol. I, no. 1, p. 447-67.
8. Mellor, M. (1967) Antarctic ice budget (and pleistocene variations of ice volume). In *The Encyclopedia of Atmospheric Sciences and Astrogeology* (R.W. Fairbridge, Ed.), Reinhold Pub. Co., p. 16-19.
9. Bentley, C.R., R.L. Cameron, C. Bull, K. Kojima and A.J. Gow (1964) Physical characteristics of the Antarctic Ice Sheet, Amer. Geograph. Soc. Antarctic Map Folio Series, Folio 2, New York.
10. Budd, W. (1977) Unpublished ANARE data.
11. Aughenbaugh, N., H. Neuburg and P. Walker (1958) Ellsworth Station glaciological and geological data, 1957-1958. Ohio State University Res. Found. Rept. 825-1, Pt. 1, USNC-IGY, p. 1-232.
12. Bender, J. and A.J. Gow (1961) Deep drilling in Antarctica. In *Symposium on Antarctic Glaciology*, Internat. Assoc. Sci. Hydrol. Pub. 55, p. 132-141.
13. Schytt, V. (1954) Glaciology in Queen Maud Land. *Geographical Review*, vol. 44, p. 70-87.
14. Wexler, H. (1960) Heating and melting of floating ice shelves. *Journal of Glaciology*, vol. 3, p. 626-45.
15. Robin, G. de Q. (1955) Ice movement and temperature distribution in glaciers and ice sheets. *Journal of Glaciology*, vol. 2, p. 523-532.
16. Gow, A.J. (1968) Deep core studies of the accumulation and densification of snow at Byrd Station and Little America V, Antarctica. CRREL Research Report 197, 45 p.
17. Tongiorgi, E., et al. (1962) Deep drilling at Base Roi Baudouin, Dronning Maud Land, Antarctica. *Journal of Glaciology*, vol. 4, p. 101-110.
18. Mellor, M. (1961) The Antarctic ice sheet. CRREL Cold Regions Science and Engineering I-B1, 50 p.
19. Mellor, M. (1964) Snow and ice on the earth's surface. CRREL CRSE II-C1, 163 p.
20. Bader, H. and D. Kuroiwa (1962) The physics and mechanics of snow as a material. CRREL CRSE II-B, 79 p.
21. Shimizu, H. (1970) Air permeability of deposited snow. Contrib. Inst. Low Temp. Sci., Ser. A, No. 22, Hokkaido Univ., 32 p.
22. Gow, A.J. (1963) The inner structure of the Ross Ice Shelf at Little America V, Antarctica, as revealed by deep core drilling. Internat. Assoc. Sci. Hydrol./Comm. of Snow and Ice Pub. 61, p. 272-84.
23. Mock, S.J. and W.F. Weeks (1966) The distribution of 10 meter snow temperatures on the Greenland Ice Sheet. *Journal of Glaciology*, vol. 6, p. 23-41.
24. Mellor, M. (1977) Engineering properties of snow. In *Symposium on Applied Glaciology, Journal of Glaciology*, vol. 19.
25. Kovacs, A., W.F. Weeks and F. Michitti (1969) Variation of some mechanical properties of polar snow, Camp Century, Greenland. CRREL Research Report 276, 33 p.
26. Mellor, M. (1964) Properties of snow. CRREL CRSE III-A1, 105 p.
27. Mellor, M. (1975) A review of basic snow mechanics. In *International Symposium on Snow Mechanics.* Internat. Assoc. Sci. Hydrol.-Internat. Comm. on Snow and Ice Pub. 114.
28. Hobbs, P.V. (1974) *Ice physics.* Clarendon Press, 837 p.
29. Glen, J.W. (1974) The physics of ice. CRREL CRSE II-C2a, 79 p.
30. Glen, J.W. (1975) The mechanics of ice. CRREL CRSE II-C2b, 43 p.
31. Gow, A.J. (1968) Electrolytic conductivity of snow and glacier ice from Antarctica and Greenland. *Journal of Geophysical Research*, vol. 73, p. 3643-49.

32. Kovacs, A. and A.J. Gow (1975) Brine infiltration in the McMurdo Ice Shelf. *Journal of Geophysical Research*, vol. 80, p. 1957-61.
33. Thomas, R.H. (1975) Liquid brine in ice shelves. *Journal of Glaciology*, vol. 14, p. 125-136.
34. Nazarov, V.S. (1962) *Ice of the Antarctic waters* (in Russian). Rezul'taty Issledovanii Po Programme Mezhdunarodnogo Geofizicheskogo Goda, *Okeanologiia*, vol. X, no. 6, Izdatel'stvo Akad, Nauk SSSR, Moscow, 79 p.
35. Gordienko, P.A. (1960) *The role of icebergs in the ice and thermal balance of coastal Antarctic waters* (in Russian). Problemy Arktiki i Antarktiki, vol. 2, p. 17-22.
36. Wordie, J.M. and S. Kemp (1933) Observations on certain Antarctic icebergs. *Geographical Journal*, vol. 81, p. 428-34.
37. Swithinbank, C. (1969) Giant icebergs in the Weddell Sea, 1967-68. *The Polar Record*, vol. 14, no. 91, p. 477-78.
38. Hult, J.L. and N.C. Ostrander (1974) Applicability of ERTS to Antarctic iceberg resources. In *Third Earth Resources Technology Satellite-1 Symposium* (S.C. Freden and M.A. Becker, Ed.), vol. IB, NASA SP-351, p. 1467-90.
39. Lebedev, V. (1959) *Antarctica*. Foreign Languages Publishing House, Moscow.
40. Kovacs, A. (1978) Iceberg thickness and crack detection. In *First International Conference on Iceberg Utilization* (A. Husseiny, Ed.), Pergamon Press.
41. Robe, R.Q., D.C. Maier and R.C. Kollmeyer (1977) Iceberg deterioration. *Nature*, vol. 267, no. 5611, p. 505-6.
42. Assur, A. (1963) Break-up of pack-ice floes. In *Ice and snow, processes, properties, and applications* (W.D. Kingery, Ed.), MIT Press, p. 335-47.
43. Zwally, H.J. and P. Gloersen (1977) Passive microwave images of the polar regions and research applications. *Polar Record*, vol. 18, no. 116, p. 431-450.
44. Campbell, W.J., R.O. Ramseier, W.F. Weeks and P. Gloersen (1976) An integrated approach to the remote sensing of floating ice. In *Proc. XXVI Internat. Astronaut. Congress* (L.G. Napolitano, Ed.), Pergamon Press, p. 445-487.
45. Griffin, O.M. (1978) Heat, mass and momentum transfer effects on the ablation of icebergs in seawater. In *First International Conference on Iceberg Utilization* (A. Husseiny, Ed.), Pergamon Press.
46. Ashton, G.D. (1972) Turbulent heat transfer to wavy boundaries. In *Proc. 1972 Heat Transfer and Fluid Mechanics Inst.* (R.B. Landis and G.J. Hordemann, Ed.), Stanford Univ. Press, p. 200-213.
47. Williams, D.T. (1963) Terminal shapes of ablating bodies. *AIAA Journal*, vol. 1, p. 494-6.
48. Mellor, M. (1975) Controlled perimeter blasting in cold regions. CRREL Technical Report 267, 24 p.
49. Mellor, M. (1976) Controlled perimeter blasting in cold regions. In *Conf. on Explosives and Blasting Techniques*, Louisville, Kentucky, Society of Explosives Engineers, 22 p.
50. Mellor, M. and A. Kovacs (1972) Destruction of ice islands by explosives. Technical Report for Arctic Petroleum Operators Assoc. (proj. operator Gulf Oil, Canada, Ltd.), 40 p.
51. Mellor, M., A. Kovacs and J. Hnatiuk (1977) Destruction of ice islands with explosives. In *POAC 77, Fourth Internat. Conf. on Port and Ocean Engineering Under Arctic Conditions*, St. John's, Newfoundland, 13 p.
52. Livingston, C.W. (1960) Explosions in ice. SIPRE Technical Report 75, 50 p.

☆U.S. GOVERNMENT PRINTING OFFICE: 1977—702-415/341